FEATURE ARTICLE

Dynamics of Nonadiabatic Chemical Reactions

Hiroki Nakamura

Institute for Molecular Science, National Institutes of Natural Sciences, Myodaiji, Okazaki 444-8585, Japan

Received: June 12, 2006; In Final Form: July 14, 2006

New methods are proposed to treat nonadiabatic chemical dynamics in realistic large molecular systems by using the Zhu−Nakamura (ZN) theory of curve-crossing problems. They include the incorporation of the ZN formulas into the Herman−Kluk type semiclassical wave packet propagation method and the trajectory surface hopping (TSH) method, formulation of the nonadiabatic transition state theory, and its application to the electron transfer problem. Because the nonadiabtic coupling is a vector in multidimensional space, the one-dimensional ZN theory works all right. Even the classically forbidden transitions can be correctly treated by the ZN formulas. In the case of electron transfer, a new formula that can improve the celebrated Marcus theory in the case of normal regime is obtained so that it can work nicely in the intermediate and strong electronic coupling regimes. All these formulations mentioned above are demonstrated to work well in comparison with the exact quantum mechanical numerical solutions and are expected to be applicable to large systems that cannot be treated quantum mechanically numerically exactly. To take into account another quantum mechanical effect, namely, the tunneling effect, an efficient method to detect caustics from which tunneling trajectories emanate is proposed. All the works reported here are the results of recent activities carried out in the author's research group. Finally, the whole set of ZN formulas is presented in Appendix.

I. Introduction

Without doubt nonadiabatic dynamics play crucial roles in physics, chemistry and biology, even if this fact is not explicitly well recognized in some occasions.[1−8] A nonadiabatic transition presents a very basic mechanism not only to comprehend various dynamic processes occurring in nature but also to manifest new molecular functions in nanospace and to control dynamic processes by applying an external field. Theory of nonadiabatic transition can play important roles to accomplish these studies. A complete set of analytical formulas for the curve-crossing problem derived by Zhu and Nakamura (Zhu−Nakamura (ZN) theory)[1,2,9−13] is actually useful for these studies.

For the creation of new molecular functions, for instance, the intriguing phenomenon of complete reflection found in the nonadiabatic tunneling type of transition in which the two diabatic potential curves cross with opposite signs of slopes may play important roles.[14,15] As for the control of chemical dynamics, nonadiabatic transitions created by an external field like laser can be manipulated by appropriately designing the field parameters so that the desirable products can be efficiently produced.[16−22] These subjects, i.e., manifestation of molecular functions and control of chemical dynamics, are not discussed in this Feature Article. This Feature Article describes a summary of the recent activities done in the author's research group concerning the first subject mentioned above, namely, the comprehension of nonadiabatic chemical reaction dynamics.

The ZN theory can be incorporated into various simulation methods to treat realistic molecular systems. Because the nonadiabatic coupling is a vector and thus we can always determine the relevant one-dimensional direction of the transition in multidimensional space, the one-dimensional ZN theory can be usefully utilized. Besides, the comprehension of reaction mechanisms can be enhanced by using the theory, because the formulas are given in simple analytical expressions. Considering the nonfeasibility of full quantum mechanical numerical simulations of realistic large systems, it would be appropriate to incorporate the theory into some kind of semiclassical methods. The promising semiclassical methods are (i) the initial value representation method[23] and (ii) the frozen Gaussian propagation method.[24−26] These methods have been developed for the adiabatic processes, namely, for the dynamics on a single adiabatic potential energy surface. Incorporation of the ZN theoy can extend the methods so as to treat electronically nonadiabatic dynamics beyond the perturbative treatment.[25,27] A much simpler simulation method is the trajectory surface hopping (TSH).[28,29] This is a classical trajectory method with electronic transitions between the two potential energy surfaces treated by the Landau−Zener formula or by solving the time-dependent coupled equations. After these original works many modifications and improvements have been introduced[30,31] and the widely spread applications have been made because of the simplicity.[32−34] However, some crucial problems have been left unsolved such as how to deal with the classically forbidden nonadiabatic transitions and how to define classical trajectories uniquely. These defects can be removed by using the ZN theory in the *adiabatic* state representation.

The ZN formulas can also be utilized to formulate a theory for the direct evaluation of the thermal rate constant of electronically nonadiabatic chemical reactions based on the idea of transition state theory.[35] This formulation can be further

10.1021/jp063643v CCC: $33.50
Published on Web 08/22/2006

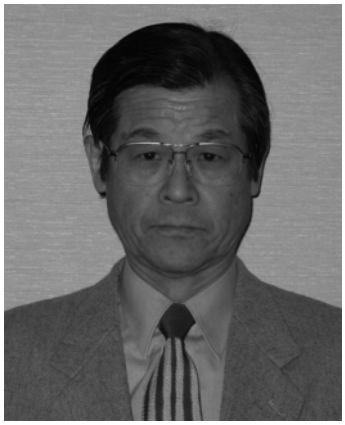

Education (undergraduate): Department of Applied Physics, The University of Tokyo, 1963. Previous position: Professor of Institute for Molecular Science (IMS). Current position: Director General of IMS, Executive Director and Vice President of NINS(National Institutes of Natural Sciences, Scientific interests: theory of chemical dynamics, semiclassical theory, nonadiabatic transition.

utilized to formulate a theory of electron transfer and an improvement of the celebrated Marcus formula can be done.[36]

Needless to say, multidimensional tunneling is another important quantum mechanical effect that should also be incorporated into simulations such as those mentioned above. To do that, the so-called caustics, which are nothing but turning points in the case of an ordinary one-dimensional system and from which tunneling trajectories emanate, should be properly detected along classical trajectories. An efficient method to do this has recently been devised by Oloyede et al.[37] This can be done by solving the first-order Riccati type time-dependent differential equation along trajectories and the method can be incorporated into the above-mentioned simulation methods.

This paper is organized as follows. Incorporation of the ZN formulas into the semiclassical frozen Gaussian wave packet propagation method and the TSH method will be described in sections II and III, respectively. Some numerical examples will be presented. The theory of nonadiabatic thermal rate constant and its application to electron transfer will be discussed in section IV. Finally, the detection of caustics will be explained in section V together with some numerical demonstrations. Section VI concludes the paper.

II. Semiclassical Herman−Kluk Type Frozen Gaussian Wave Packet Propagation Method

As mentioned above, full quantum mechanical treatments are limited only to low dimensional systems and it is desirable to develop effective semiclassical theories with nonadiabatic transitions incorporated. In the adiabatic state representation a whole chemical process can be divided into the following two steps (see Figure 1): (i) motion on a single adiabatic potential energy surface up to the region of nonadiabatic transition and (ii) nonadiabatic transition at the potential surface crossing. As mentioned above, there are two types of semiclassical path integral methods for the propagation on a single potential energy surface. One is the initial value representation theory with use of classical trajectories devised by Miller and others.[23] In this case the nonadiabatic transition amplitude of the ZN theory can be directly incorporated into the framework. The other is the frozen Gaussian wave packet propagation method.[24−26] The Herman−Kluk propagator combined with the cellularization procedure works well, giving good agreement with full quantum calculations.[25,26] The semiclassical approach explained in this section makes use of the advantages of the Herman−Kluk theory

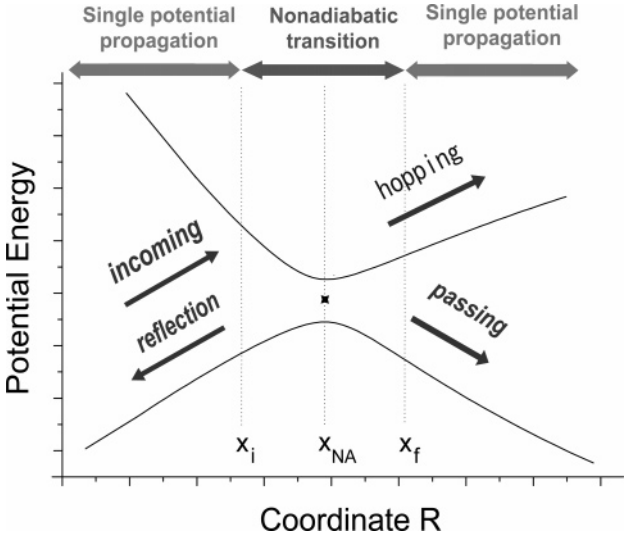

Figure 1. Two basic elements of dynamics: (i) propagation on a single potential and (ii) nonadiabatic transition. In the classically allowed case, the nonadiabatic transition occurs at X_{NA}. In the classically forbidden case, the transition region spans the interval (x_i, x_f), where x_i and x_f correspond to the turning points.

for single surface propagation[25] and the ZN theory for nonadiabatic transition. The nonadiabatic transition amplitude of the ZN theory properly provides also the so-called dynamical phases induced by the nonadiabatic transition and can be incorporated into each frozen Gaussian wave packet by expanding the latter in terms of energy normalized eigenstates.

Here only the outline of the formulation is described so that the reader can grasp the essential ideas of the method. The details of the formulation can be found in the original papers.[27,38] The total wave function at time t in the Herman−Kluk approach is expressed as

$$\psi(\mathbf{r},t) = \int_{\text{traj}} \frac{d\mathbf{q}_0\, d\mathbf{p}_0}{(2\pi)^N} g(\mathbf{r};\mathbf{q}_t,\mathbf{p}_t) C_{\mathbf{q}_0,\mathbf{p}_0 t} \times \exp[iS_{\mathbf{q}_0,\mathbf{p}_0,t}] \int d\mathbf{r}_0\, g^*(\mathbf{r}_0;\mathbf{q}_0,\mathbf{p}_0)\, \psi(\mathbf{r}_0,t=0) \quad (1)$$

where $\psi(\mathbf{r}_0,t=0)$ and $\psi(\mathbf{r},t)$ are the wave functions at time zero and t, respectively, N is the dimensionality of configuration space, $S_{\mathbf{q}_0,\mathbf{p}_0,t}$ is the classical action along the trajectory from $(\mathbf{q}_0,\mathbf{p}_0,t=0)$ to $(\mathbf{q}_t,\mathbf{p}_t,t)$, and $C_{\mathbf{q}_0,\mathbf{p}_0,t}$ is the Herman−Kluk preexponential factor along the trajectory.[25] The frozen Gaussian wave packes are defined as

$$g(\mathbf{r};\mathbf{q},\mathbf{p}) = \left(\frac{2\gamma}{\pi}\right)^{N/4} \exp[-\gamma(\mathbf{r}-\mathbf{q})^2 + i\mathbf{p}\cdot(\mathbf{r}-\mathbf{q})] \quad (2)$$

where γ is a constant parameter common for all wave packets. The above expression for $\psi(\mathbf{r},t)$ is explained as follows: the initial wave function is expanded in terms of the frozen Gaussian wave packets and each packet is propagated by classical mechanics with its shape kept fixed. The final wave function is expressed as a sum of thus propagated frozen wave packets multiplied by the factor $C_{\mathbf{q}_0,\mathbf{p}_0,t} \exp[iS_{\mathbf{q}_0,\mathbf{p}_0,t}]$. The initial parameters ($\mathbf{q}_0$, $\mathbf{p}_0$) of trajectories are selected by the well-established Monte Carlo procedure. This propagation is made on a single adiabatic potential energy surface and is carried out up to the region of potential energy surface crossing. It is assumed that the nonadiabatic transition occurs locally and instantaneously at the position $\mathbf{q}_I$ where the adiabatic potential energy difference becomes minimum along the trajectory. Once this transition position is found, the nonadiabatic transition is taken into

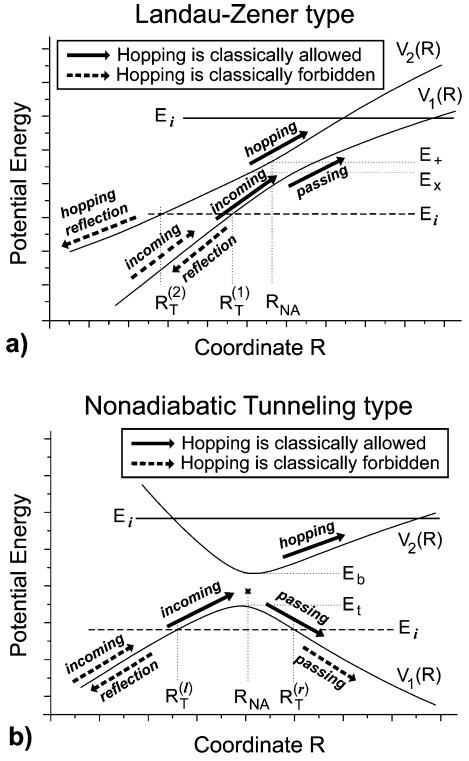

Figure 2. Interpretation of the mode: reflection, passing and hopping. $V_1(R)$ and $V_2(R)$ represent adiabatic potentials. Reprinted with permission from ref 27. Copyright 2004 American Institute of Physics.

account as follows. The local separability in the vicinity of $\mathbf{q}_I$ is assumed and the one-dimensional direction of transition is determined. If the nonadiabatic coupling vector is available, the one-dimensional cut is made along that direction. If it is not available, we can determine the direction from the Hessian there.[39] If the geometry of the potential energy surface-crossing seam is known in advance, we can take the direction perpendicular to the seam surface. By using one of these methods, we can reduce the problem to the one-dimensional one and apply the ZN theory.

First, the frozen Gaussian wave packets just before the transition on the initial adiabatic surface i are expanded as

$$g_I(\mathbf{r};\mathbf{q}_I,\mathbf{p}_I,t) = \int dE\ \alpha^i(E)\ \phi^i(E,\mathbf{r}) \tag{3}$$

where $\{\phi^i(E,\mathbf{r})\}$ are the energy normalized eigenfunctions in the electronic state i at $\mathbf{q} \sim \mathbf{q}_I$. Right after the transition the coefficient $\alpha^i(E)$ changes to

$$\alpha^f_m(E) = T^m_{fi}\alpha^i(E) \tag{4}$$

where f and m specify the final electronic state and the mode on that state, respectively. The mode specifies one of the following three:reflection, passing, or hopping (see Figure 2). Namely, the coefficient T^m_{fi} represents the transition amplitude for the reflection or passing on the same adiabatic potential energy surface as the initial one, f = i, or hopping to the other potential energy surface, f ≠ i, after the transition, and is directly given by the ZN formulas including dynamical phases.

The final wave function $\varphi^f(\mathbf{r})$ right after the transition is thus given by

$$\varphi^f(\mathbf{r}) = \sum_m \int dE\ \alpha^f_m(E)\ \phi^f(E,\mathbf{r}) \tag{5}$$

where $\{\phi^f(E,\mathbf{r})\}$ are the energy eigenfunctions in the final electronic state f. The function $\varphi^f(\mathbf{r})$ is expanded in terms of the frozen Gaussian wave packets $g_f(\mathbf{r};\mathbf{q}_F,\mathbf{p}_F)$ of the same shape as before and the expansion coefficients F_{fi} are given by

$$F_{fi}(\mathbf{q}_F,\mathbf{p}_F,\mathbf{q}_I,\mathbf{p}_I) = \int d\mathbf{r}\ g^*_F(\mathbf{r};\mathbf{q}_F,\mathbf{p}_F)\ \varphi^f(\mathbf{r},\mathbf{q}_F,\mathbf{p}_F:\mathbf{q}_I,\mathbf{p}_I) \tag{6}$$

where $\mathbf{q}_F$ and $\mathbf{p}_F$ are the position and momentum right after the transition. The position $\mathbf{q}_F$ is not necessarily the same as $\mathbf{q}_I$, because in the case of classically forbidden transition when the energy E is lower than the crossing point, the positions $\mathbf{q}_I$ and $\mathbf{q}_F$ are turning points on the respective potential energy curve and are different from each other. The frozen Gaussian wave packets $g_F(\mathbf{r};\mathbf{q}_F,\mathbf{p}_F)$ are further propagated on the potential energy surface f. Then the final wave function at time t after the transition is expressed as

$$\psi_f(\mathbf{r},t) = \int_{traj}\frac{d\mathbf{q}_0\mathbf{p}_0}{(2\pi)^N}\int_{traj}\frac{d\mathbf{q}_F\,d\mathbf{p}_F}{(2\pi)^N} g_F(\mathbf{r};\mathbf{q}_t,\mathbf{p}_t)C_{\mathbf{q}_F,\mathbf{p}_F,t} \times \exp[iS_{\mathbf{q}_F,\mathbf{p}_F,t}]F_{fi}(\mathbf{q}_F,\mathbf{p}_F,\mathbf{q}_I,\mathbf{p}_I)C_{\mathbf{q}_0,\mathbf{p}_0,t_{NA}} \times \exp[iS_{\mathbf{q}_0,\mathbf{p}_0,t_{NA}}]\int d\mathbf{r}_0\ g^*_I(\mathbf{r}_0;\mathbf{q}_0,\mathbf{p}_0)\ \psi_i(\mathbf{r}_0,t=0) \tag{7}$$

where t_{NA} represents the time of nonadiabatic transition and $(\mathbf{q}_t, \mathbf{p}_t)$ are the coordinate and mometum at time t of the trajectory started from $(\mathbf{q}_F, \mathbf{p}_F)$. In the actual computations the integrals with respect to $\mathbf{q}_F$ and $\mathbf{p}_F$ are replaced by the sum of the main components of the wave packets right after the transition.[27,38] The analysis of the function $|F_{fi}(\mathbf{q}_F,\mathbf{p}_F,\mathbf{q}_I,\mathbf{p}_I)|$ indicates that the main components can be found from the general principle of nonadiabatic transition in the one-dimensional system.

Numerical examples are shown in Figures 3 and 4.[38] This is a two-dimensional H_2O model system in a continuous wave (CW) laser field of wavelength 300 nm (about 4.1 eV). The laser intensity is 10^{13} W/cm^2. The bending and rotational motions are neglected with the bending angle fixed at the equilibrium position, i.e., 104.52°. The potential enegy surfaces of the ground and first excited states and the transition dipole moment are the same as those in.[40] Initial wave packet is a symmetric Gaussian of the full width at half-maximum 0.5 au centered at $\mathbf{R} = (5.0\text{ au}, 3.0\text{ au})^T$ on the upper adiabatic potential energy surface. Because the Floquet or dressed-state representation is used, the upper adiabatic state corresponds to the dressed *ground* state and the process mimics the photodissociation. The mean momentum of the initial wave packet is zero. Figure 3 shows the two potential energy surfaces, and Figure 4 presents a comparison between the present semiclassical resutls (Figure 4b,d) and the exact quantum mechanical numerical solutions (Figure 4a,c). The semiclassical method works well. The final population on the excited state, namely the photodissociation probability, is 29% in the semiclassical approximation in comparison with 35% of the excat quantum result. The propagation period and the number of trajectories used are 20 fs and 7000, respectively.

A method similar to that mentioned above can be applied to laser control of chemical dynamics. We have recently formulated a semiclassical optimal control theory based on the gradient search method[41] in which the time correlation function composed of the forward and backward time-dependent wave functions is the basic quantity to be evaluated.[38,42] This semiclassical theory can now deal with realistic systems with more than three degrees of freedom[42] that cannot be teated by the full quantum optimal control theory.[16] Here we do not go

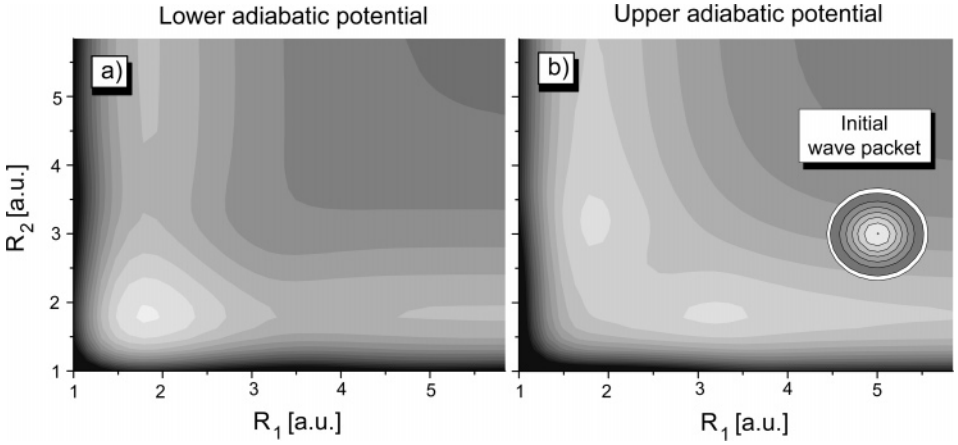

Figure 3. Two-dimensionalmodel potentials of H_2O in the dressed state picture. The upper adiabatic potential is thus the dressed ground state. Reprinted with permission from ref 21. Copyright 2005 World Scientific Publishing Co.

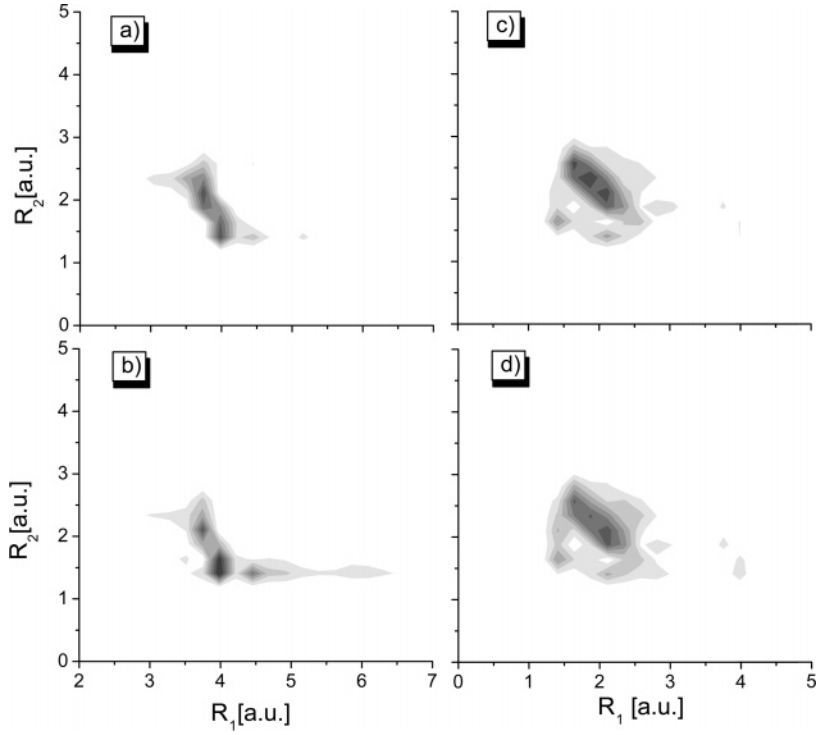

Figure 4. Final wave packets after photodissociation. (a) and (c): quantum mechanical numerical solutions of coupled Schroedinger equations. (b) and (d): corresponding semiclassical results. (a) and (b): on the ground state. (c) and (d): on the excited state. Reprinted with permission from ref 21. Copyright 2005 World Scientific Publishing Co.

into the details about this and the reader should refer to the above references.

III. Generalized Trajectory Surface Hopping Method

The simplest method to treat nonadiabatic dynamics is the trajectory surface hopping (TSH) method introduced by Bjerre and Nikitin[28] and by Tully and Preston,[29] in which classical trajectories hop at the potential energy surface crossing according to the nonadiabatic transition probability evaluated by the Landau−Zener formula or the solution of time-dependent coupled equations. At each occasion a random number is generated and the nonadiabatic surface hopping is made, if the calculated probability is larger than the random number (anteater procedure). Because of its simplicity the method is applicable to large systems and has enjoyed widespread applications.[32−34] Various modifications from the original version have been made especially by Tully and by Truhlar and co-workers.[30,31] There still remain, however, some crucial problems related to (i) definition of classical trajectory, (ii) localizability of the transition, (iii) energy and angular momentum conservation, and (iv) treatment of classically forbidden transition in which the energy is lower than the energy at surface-crossing point. In the *adiabatic* state representation, a classical trajectory runs on a single adiabatic potential energy surface until it reaches the surface-crossing region and the nonadiabatic transition can be assumed to occur locally there. In this case it is not conveneint to solve the time-dependent coupled equations to estimate the transition probability. The time-dependent coupled equations convenient to solve are given in the *diabatic* state representation, in which the localizability of the transition cannot hold well and the unique definition of classical trajectory becoms questionable. If one uses the Landau−Zener formula in the *adiabatic* representation, these problems are not very serious; but the Landau−Zener formula does not work well when the energy is

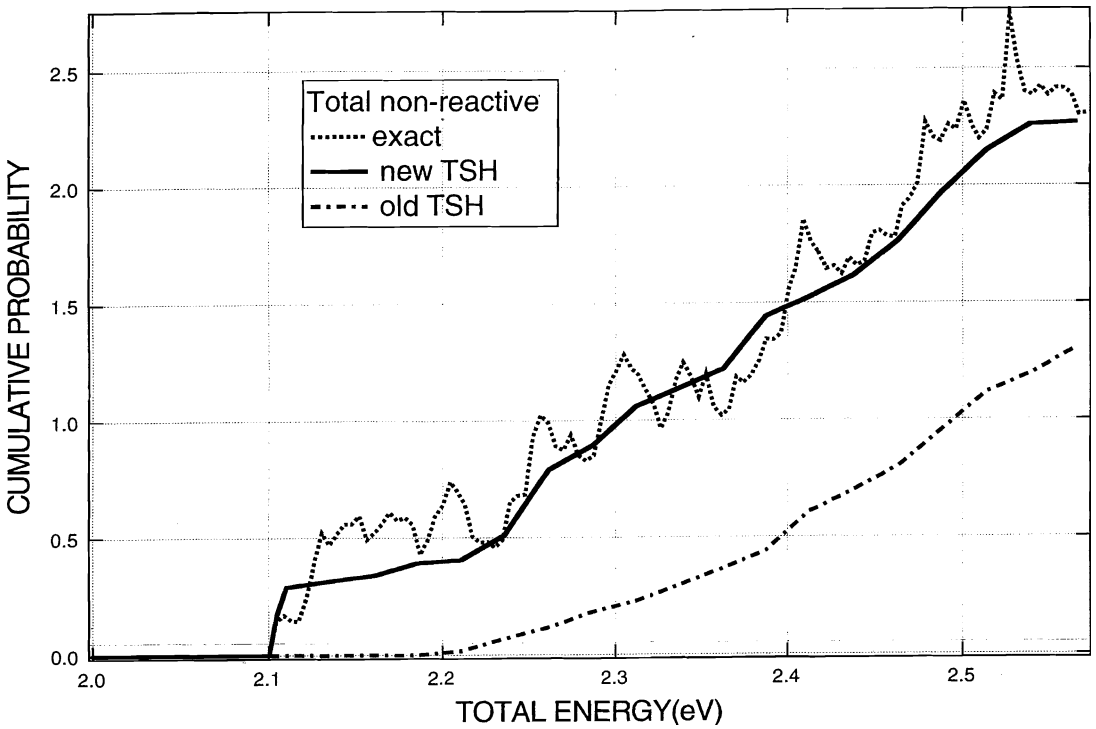

Figure 5. Total cumulative charge-transfer probabilities for $H_2 + D^+ \rightarrow H_2^+ + D$. Dashed line: exact quantum mechanical numerical solution. Solid line: TSH results with use of the Zhu−Nakamura formulas. Dash−dot line: TSH results with use of the Landau−Zener formula. Reprinted with permissino from ref 43. Copyright 2001 American Institute of Physics.

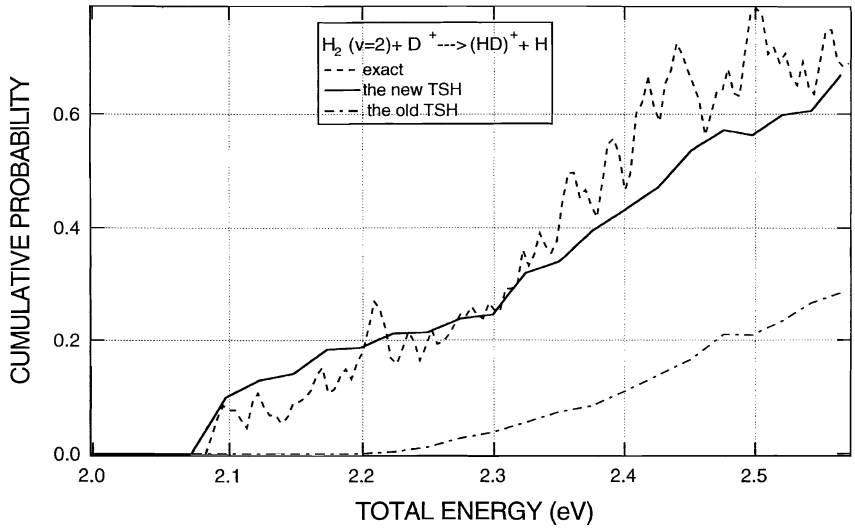

Figure 6. Initial vibrational state specified cumulative reaction probabilities for $v = 2$. Dashed line: exact quantum mechanical numerical solution. Solid line: TSH results with use of the Zhu−Nakamura formulas. Dash−dot line: TSH results with use of the Landau−Zener formula. Reprinted with permission from ref 43. Copyright 2002 American Institute of Physics.

close to the surface-crossing energy. The most serious problem is that the classically forbidden transitions cannot be treated by any one of these methods. It is well-known that the Landau−Zener formula cannot treat those transitions, but even the solutions of the time-dependent coupled equations and the widely used fewest switches method of Tully[30] cannot properly take into accout those classically forbidden transitions.

If we employ the ZN formulas in the *adiabatic* state representation, all the problems mentioned above can be solved. Because the localizability holds well, classical trajectories can run on a single adaiabatic potential energy surface and thus the effects of relaxation can be taken into account easily. We have first applied the ZN formulas to the DH_2^+ system and demonstrated that the method works well in comparison with the exact quantum mechanical numerical solutions.[43] Importance of the classically forbidden transitions has been clearly demonstrated. The Landau−Zener formula gives a bit too small results even at high energies. It was found that in multidimensional systems classically forbidden transitions play relatively more important roles than in the case of one-dimension because of energy transfer among many degrees of freedom. Some of the results are shown in Figures 5 and 6. The quantum results show violent oscillations which are resonances due to the potential well of the ground state. In the TSH calculations all the long lived trajectories are killed, because we are not interested in resonances here. This reaction system is, however, a relatively simple one, because the surface-crossing seam exists a bit away from the reaction zone, only the Landau−Zener type of crossing in which the two diabatic potential curves have the same sign of slopes appears, and the geometry of the seam

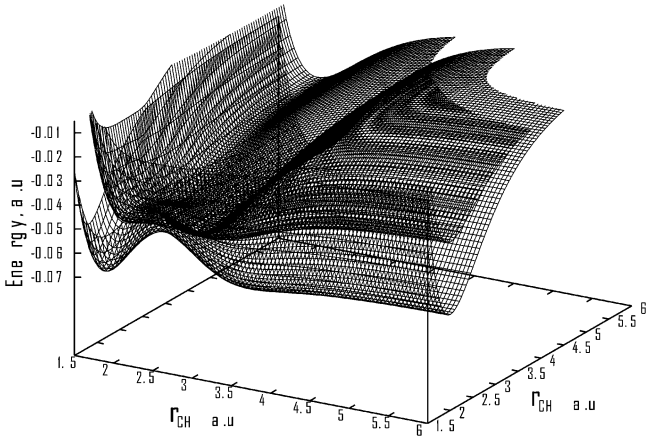

Figure 7. Adiabatic potential energy surfaces for the DIM model of CH_2 at the HCH angle fixed at 110°. Reprinted with permission from ref 39. Copyright 2006 American Institute of Physics.

surface can be well defined. Recently, we have generalized this method so that it can be applied to any general large systems.[39]

The method is composed of the following algorithms: (i) the transition position is detected along each classical trajectory, (ii) the direction of transition is determined there and the one-dimensional cut of the potential energy surfaces is made, (iii) judgment is made whether the transition is Landau−Zener type or nonadiabatic tunneling type, and (iv) the transition probability is calculated by the appropriate ZN formula. The transition position can be simply found by detecting the minimum energy separation between the two adiabatic potential energies. The determination of transition direction has the following options as mentioned in the previous section: (a) direction perpendicular to the seam surface, if the latter can be well defined in advance; (b) direction of the nonadiabatic coupling vector, if it is available; (c) direction estimated from the Hessian. If the seam surface is known well, method a is the best, because the nonadiabatic transition in the direction parallel to the seam surface is the so called Rosen−Zener type and can usually be neglected. In general, however, the geometry of the seam surface cannot be known in advance. The second best in that case is the direction of the nonadaiabtic coupling vector. However, the vector is not necessarily available, in general, unfortunately. In such a case, the last choice is to take the direction of the eigenvector of the only nonzero eigenvalue of the rank one Hessian matrix of the difference between the two adiabatic potential energy surfaces.[39] In the case of classically forbidden transitions, the nonadiabatic transition and the nuclear tunneling

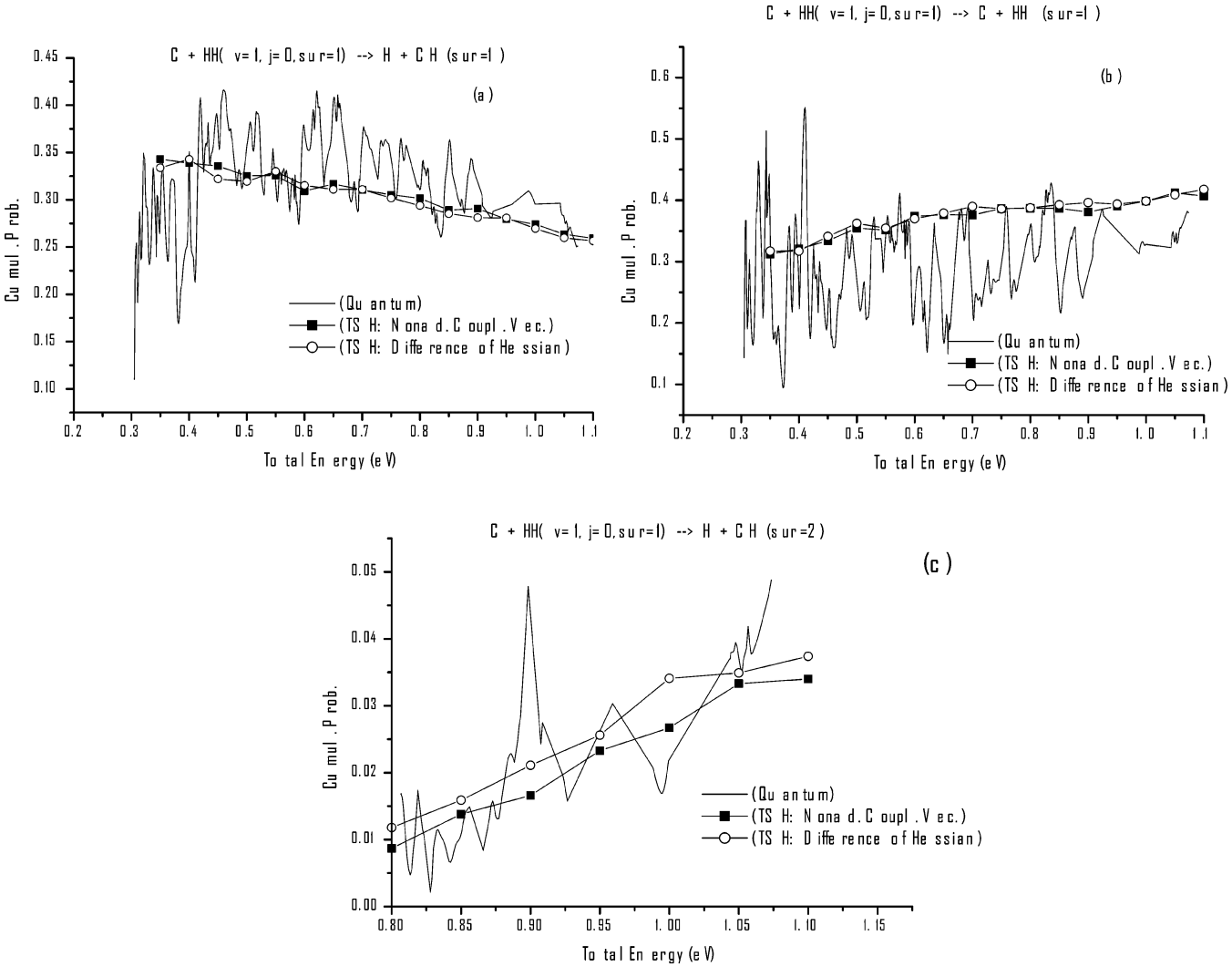

Figure 8. Initial rovibrational state specified reaction probabilities. Solid line: exact quantum mechanical numerical solution. Solid line with solid square: generalized TSH with use of nonadiabatic coupling vector. Solid line with open circle: generalized TSH with use of Hessian. Reprinted with permission from ref 39. Sur=1(2) in the figure means the ground (excited) potential energy surface. Copyright 2006 American Institute of Physics.

are coupled; i.e., they cannot be treated separately. Besides, the transitions are not vertical anymore. The ZN formulas properly describe the nonvertical transitions and provide the overall transition probability. The position right after the transition is not equal anymore to the position before the transition. The total angular momentum conservation apparently violated by the nonvertical transition can be recovered by appropriately rotating the system. The detailed recipe is not described here but can be found in ref 39. The energy conservation is not a problem at all, because the classically forbidden transitions are treated properly and the total energy after the transitions is conserved.

This generalized TSH (ZN-TSH) has been applied to a model triatomic system mimicking CH_2, which has a conical intersection, and both Landau−Zener and nonadiabatic tunneling types of transitions appear.[39] The ground and excited potential energy surfaces are constructed by using the DIM (diatomics in molecule) method (see Figure 7). The numerical results in comparison with the excat quantum mechanical numerical solutions are shown in Figure 8. The oscillations in the quantum results are again resonances due to the attractive well in the ground state. Apart from these oscillations the ZN-TSH works acceptably well. In these figures the two ZN-TSH results are compared with respect to the choice of the transition direction: (i) the direct use of nonadiabatic coupling vector and (ii) the Hesssian approximation. It is clearly seen that the Hessian approximation works well. These successful demonstrations confirm the potentiality of applying the present method to general large systems of general potential energy surface topology. With the present method the very popular classical mechanical MD (molecular dynamics) simulation method could be easily improved and extended so as to take into account the nonadiabatic transitions properly. Finally, it would be worthwhile to mention that another important quantum mechanical effect, namely, quantum mechanical tunneling, can also be taken into account in the present methodology. To do that, it is crucial to detect caustics (turning points in one-dimensional case) along trajectories. This can be easily done, as will be explained later in section 5.

IV. Semiclassical Theory of Nonadiabatic Thermal Rate Constant and Electron Transfer

Another interesting subject is the direct evaluation of thermal rate constants for electronically nonadiabatic chemical reactions. "Direct" means not from the detailed scattering matrix calculations, as has been well discussed by Miller and co-workers for the single surface adiabatic processes.[44,45] Extending the trace formula by Miller, we have formulated the thermal rate constant for nonadiabatic reactions with use of the Zhu−Nakamura formulas.[35,46] In the simple case that the transition state is created by the nonadiabatic tunneling type surface crossing, we have derived a simple formula by explicitly considering the geometry of crossing seam surface and the coordinate-dependent nonadiabatic transition probability on that.[35] The formula was demonstrated to work well in the case of one- and two-dimensional model systems and is expected to be applicable to high dimensional systems with use of the Monte Carlo sampling method.

We start with the rigorous quantum mechanical rate contant in terms of the flux−flux correlation function:[47]

$$kZ_r = \lim_{t\to\infty} \mathrm{Tr}[\exp(-\beta H)F \exp(\mathrm{i}Ht/\hbar)h \exp(-\mathrm{i}Ht/\hbar)] \quad (8)$$

where Z_r is the partition function of the reactant, h is the Heaviside step function, and $F = (\mathrm{i}/\hbar)[H,h]$ is the flux operator through the dividing surface defined as $S(\mathbf{Q}) = 0$, with $\mathbf{Q}$ denoting the set of mass reduced Cartesian coordinates. With use of the dividing surface $S(\mathbf{Q}) = 0$ the flux operator F can be expressed as

$$F = \mathbf{P}^{\mathrm{T}} \nabla S(\mathbf{Q})\, \delta[S(\mathbf{Q})] \quad (9)$$

where $\mathbf{P}^{\mathrm{T}}$ is the transposed momentum vector. Replacing the time-dependent Heaviside function by its classical analogue and the quantum mechanical trace by the phase space integration, we have

$$kZ_r = \frac{1}{h^{3N}} \int \mathrm{d}\mathbf{P}\, \mathrm{d}\mathbf{Q} \exp(-\beta H)\mathbf{P}^{\mathrm{T}} \nabla S(\mathbf{Q})\, \delta[S(\mathbf{Q})]\, P[E_s, S(\mathbf{Q})] \quad (10)$$

where E_s is the translational energy component perpendicular to the seam surface and the classical Heaviside function is replaced by the ZN nonadiabatic tunneling probability $P(E_s)$ at the seam surface. Carrying out the integration with respect to all the components of momentum except for p_s, which is the component normal to the seam surface and introducing the quantum mechanical corrections to the partition functions, we finally obtain

$$k = \frac{Z_q^{\dagger}}{Z_r^{q}} \sqrt{\frac{1}{2\pi\beta}} \frac{\int \mathrm{d}\mathbf{Q}\, P(\beta,\mathbf{Q}) |\nabla S(\mathbf{Q})| \delta[S(\mathbf{Q})] \exp[-\beta V(\mathbf{Q})]}{\int \mathrm{d}\mathbf{Q}\, \delta[S(\mathbf{Q})] \exp[-\beta V(\mathbf{Q})]} \quad (11)$$

where $Z_q^{\dagger}$ and Z_r^{q} are the quantum mechanical partition functions of activated complex and reactants, respectively. The effective coordinate-dependent transmission probability $P(\beta,\mathbf{Q})$ is defined by

$$P(\beta,\mathbf{Q}) = \beta \int_0^{\infty} \mathrm{d}E_s \exp(-\beta[E_s - V(\mathbf{Q})]) P(E_s,\mathbf{Q}) \quad (12)$$

The above formula has been tested by using the model collinear reaction described by the following diabatic potentials:[48]

$$V_1(r,R) = D(1 - \exp[-\beta(r - r_e)])^2 + \frac{1}{2}D\left(1 + \exp\left[-\beta\left(R + \frac{1}{2}r - r_e\right)\right]\right)^2 - \frac{1}{2}D \quad (13)$$

$$V_2(r,R) = D\left(1 - \exp\left[-\beta\left(R - \frac{1}{2}r - r_e\right)\right]\right)^2 + \frac{1}{2}D\left(1 + \exp\left[-\beta\left(R + \frac{1}{2}r - r_e\right)\right]\right)^2 - \frac{1}{2}D \quad (14)$$

$$V_c(r,R) = A \exp(-\gamma[(r - r_e)^2 + (R - R_c)^2]) \quad (15)$$

where V_c is the diabatic coupling between the two potentials and the parameters used are $D = 4.9$ eV, $\beta = 1.877$ Å, $r_e = 0.7417$ Å, $r_c = 1.5707$ Å, $R_c = 1.5r_c$,$\gamma = 0.01$ Å^{-2} and $A = 0.1$ eV. Figure 9 shows the contour plot of the adiabatic ground state in the mass reduced coordinates.

Figure 10 shows the Arrhenius plot of the numerical results of the thermal rate constants. The solid circles are the exact quantum mechanical numerical solutions. The thick solid line represents the results of the present formulation, namely the results of eq 11. The thin solid line is the result of using the classical partition function instead of using the proper quantum one. It is clearly seen that the quantum correction of the partition function is important. The dashed lines are the results of the

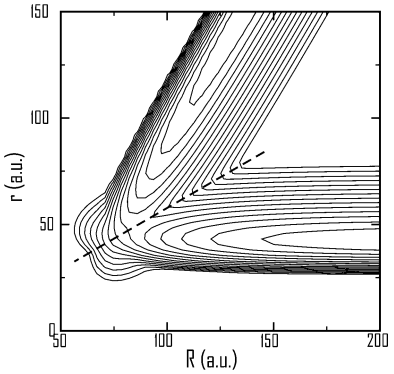

Figure 9. Contour plot of the ground adiabatic potential energy surface for the 2D model. The dash line represnts the seam surface. Reprinted with permission from ref 35. Copyright 2004 American Institute of Physics.

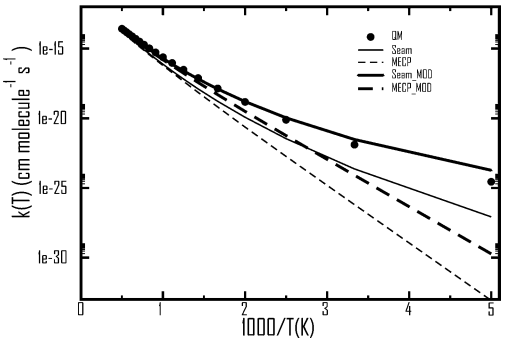

Figure 10. Arrhenius plot of the thermal rate constants for the 2D model. Solid circle: exact quantum mechanical numerical solution. Thick solid line: present nonadiabatic TST. Thick dashed line: present nonadiabatic TST with use of the minimum energy crossing point (MECP) approximation. Thin solid line: present nonadiabatic TST without the quantum mechanical correction to the partition function. Thin dashed line: present nonadiabatic TST with use of MECP without the quantum mechanical correction to the partition function. Reprinted with permission from ref 35. Copyright 2004 American Institute of Physics.

conventional transition state approximation in which the transmission probability is calculated only at the minimum energy crossing point (MECP) and its coordinate dependence is neglected. The thin (thick) dashed line corresponds to the results using the classical (quantum) partition function. These test calculations clearly demonstrate that the present formulation gives correct estimates, if the coordinate-dependent nonadiabatic tunneling transition probability and the quantum mechanical correction of the partition function are properly taken into account.

The present treatment is quite a simple one and the following two generalizations are naturally required: (i) applications to multidimensional complicated molecular systems, and (ii) formulation applicable to a more general case that the ordinary transition state and the potential surface crossing are separated. The former may be done without difficulty by using the well-established Monte Carlo technique. The latter case requires a somewhat new formulation and now is in progress.[46]

Electron transfer, which is a very important process in chemistry and biology,[49,50] can be a nice subject to be treated by the present theory. Not only in the original Marcus theory but also in the conventional treatments of electron transfer is the electronic coupling dealt with by the perturbation theory or by the Landau−Zener formula. Now we know that the intermediate to strong diabatic coupling cases and the classically forbidden transitions cannot be properly described by these treatments. It is natural to think about incorporation of the ZN formulas into the theories of electron transfer. The first step to do this is to reformulate the famous Marcus formula under the assumption of thermally activated process with the fast dielectric relaxation. This was done in ref 36. Here, we consider only the so-called normal case that corresponds to the nonadiabatic tunneling type of potential crossing and present only the essential portion of the formulation together with some numerical results. We can start from eq 11. Because the electron-transfer rate is described in the representation of free energy, we introduce the free energy by

$$\exp[-\beta F_1(\xi)] = \int \mathrm{d}\mathbf{Q}\, \exp[-\beta V_1(\mathbf{Q})]|\nabla S(\mathbf{Q})|\delta(\xi - S(\mathbf{Q})) \tag{16}$$

and rewrite the thermal rate constant as

$$k = \frac{Z_{\mathrm{q}}^{\dagger}}{Z_{\mathrm{r}}^{\mathrm{q}}} Z_{\mathrm{cl}}^{-1} \sqrt{\frac{1}{2\pi\beta}}\, \bar{P}(\beta,\xi_0) \int \mathrm{d}\xi\, \delta(\xi - \xi_0) \exp[-\beta F_1(\xi)] \tag{17}$$

where Z_{cl} is the denominator in eq 11 and the average transition probability $\bar{P}(\beta,\xi)$ is defined by

$$\bar{P}(\beta,\xi) = \frac{\int \mathrm{d}\mathbf{Q}\, \exp[-\beta V_1(\mathbf{Q})]|\nabla S(\mathbf{Q})|\delta(\xi - S(\mathbf{Q}))\, P(\beta,\mathbf{Q})}{\int \mathrm{d}\mathbf{Q}\, \exp[-\beta V_1(\mathbf{Q})]|\nabla S(\mathbf{Q})|\delta(\xi - S(\mathbf{Q}))} \tag{18}$$

In the linear response limit, the free energies $F_j(\xi)$ ($j = 1, 2$) of the donor and acceptor can be expressed by parabolic functions of ξ as

$$F_1(\xi) = -\frac{1}{\beta} \ln[\int \mathrm{d}\mathbf{Q}\, \exp[-\beta V_1(\mathbf{Q})]|\nabla S(\mathbf{Q})|\delta(\xi - S(\mathbf{Q}))] = \frac{1}{2}\omega^2(\xi - \xi_{01})^2 \tag{19}$$

$$F_2(\xi) = -\frac{1}{\beta} \ln[\int \mathrm{d}\mathbf{Q}\, \exp[-\beta V_2(\mathbf{Q})]|\nabla S(\mathbf{Q})|\delta(\xi - S(\mathbf{Q}))] = \frac{1}{2}\omega^2(\xi - \xi_{02})^2 + \Delta G \tag{20}$$

where ξ_{01} and ξ_{02} are the positions of the free energy minima of donor and acceptor, respectively, and ΔG represents the exothermicity of the reaction which is determined from eq 20.

From the above equations we can finally obtain

$$k = \kappa k_{\mathrm{Marcus}} \tag{21}$$

with

$$\kappa = \frac{\hbar\omega}{2\pi {H_{\mathrm{AD}}}^2} \sqrt{\frac{\lambda}{\pi\beta}}\, \bar{P}(\beta,\xi_0) \tag{22}$$

where k_{Marcus} is the Marcus formula defined by

$$k_{\mathrm{Marcus}} = \frac{{H_{\mathrm{AD}}}^2}{\hbar} \sqrt{\frac{\pi\beta}{\lambda}} \exp\left[-\frac{-\beta(\lambda + \Delta G)^2}{4\lambda}\right] \tag{23}$$

and H_{AD} is the electronic coupling between acceptor and donor. The reorganization energy λ is defined by

$$\lambda = \frac{1}{2}\omega^2(\xi_{02} - \xi_{01})^2 \tag{24}$$

The effects of nonadiabatic transition and tunneling are

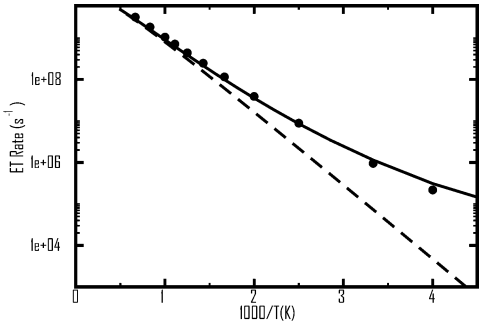

Figure 11. Arrhenius plot of the electron-transfer rate at $H_{AD} = 0.0001$ au. Solid line: Bixon−Jortner perturbation theory. Full circle: present result. Dashed line: Marcus' high temperature theory. Reprinted from ref 36.

properly taken into account by κ and the main task is to evaluate the average transition probability $\bar{P}(\beta, \xi)$ in which the nonadiabatic tunneling probability $P(E_s,\mathbf{Q})$ on the seam surface given by the ZN formula plays the essential role (see eqs 18 and 12). It should also be noted that the electronic coupling H_{AD} is assumed to be constant in the Marcus formula, but this is not necessary in the present formulation. The coupling H_{AD} cancels out in k of eq 21 and the ZN probability can be calculated from the information of adiabatic potentials (see Appendix).

The above formulation can be directly applied to multidimensional systems and its numerical results for the system of twelve harmonic oscillators are shown below. The model potentials used are

$$V_1 = \frac{1}{2}\sum_{j=1}^{12}\omega_j^2 Q_j^2 \tag{25}$$

$$V_2 = \frac{1}{2}\sum_{j=1}^{12}\omega_j^2 (Q_j - Q_{0j})^2 \tag{26}$$

where the exothermicity ΔG is taken to be zero and the parameters ω_j and the reorganization energies $\lambda_j = (\omega_j Q_{0j})^2/2$ are as follows:

ω_j ($j = 1-12$) (cm^{-1}) =
462, 511, 584, 602, 628, 677, 1007, 1169, 1252, 1334, 1403, 1548

λ_j ($j = 1-12$) (cm^{-1}) =
3038, 1372, 775, 1039, 2125, 1196, 269, 638, 351, 625, 275, 100

The reaction coordinate ξ is defined as $\xi = V_1 - V_2$ and thus the seam surface corresponds to $\xi = \xi_0 = 0$. The actual computations are carried out by using the Monte Carlo method. The results are shown in Figures 11 and 12.

Figure 11 shows the Arrhenius plot of the rate for the weak electronic coupling case ($H_{AD} = 0.0001$ au) in which the perturbation theory works. The present reults (filled circles) agree well with those of Bixon−Jortner perturbation theory (solid line)[51] over the whole temperature range, whereas the Marcus formula (dashed line) works only at high temperatures because the nuclear tunneling effect is not taken into account.

Figure 12 shows the rate against the coupling strength at temperature $T = 500$ K. The Bixon−Jortner (dash line) and Marcus (dotted line) theories break down as the electronic coupling strength increases. The MECP approximation within the present formulation (solid line with open square) agrees well with the present results without MECP (solid line with open circle). This is, however, simply because the electronic coupling

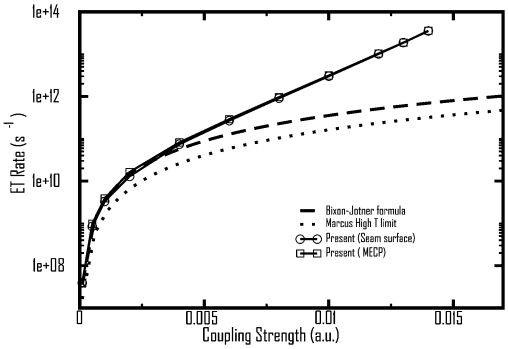

Figure 12. Electron-transfer rate against the electronic coupling strength at $T = 500$ K. Solid line with circle (square): present results without (with) the MECP approximation. Dashed line: Bixon−Jortner theory. Dotted line: Marcus' high temperature theory. Reprinted from ref 36.

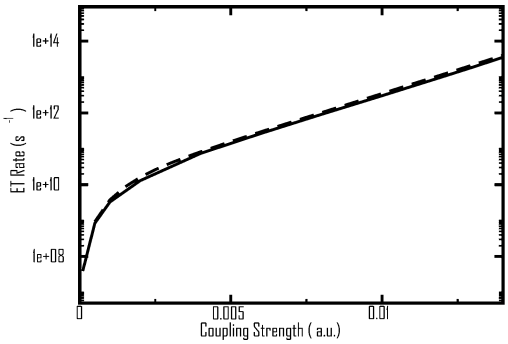

Figure 13. Electron-transfer rate against electronic coupling strength at $T = 500$ K in the symmetric potential case. Solid line: present full dimensional result. Dashed line: present result in the effective one-dimensional model. Reprinted from ref 36.

is assumed to be constant. As mentioned before, the MECP approximation is considered not to be good enough in general. It should also be noted that the present theory works all right in the case of general asymmetric potentials,[36] because the ZN formulas are valid for general curve-crossing problems.

It would be very useful and convenient for the interpretation of experimental data, if we can introduce a certain effective one-dimensional model for a collection of harmonic oscillators. Actually, this can be done to a good extent by using the method proposed by Dogonadze and Urushadze.[52] The effective one-dimensional frequency ω is defined as

$$\omega^2 = \frac{1}{\lambda}\sum_j \omega_j^2 \lambda_j \tag{27}$$

The corresponding potentials are given by

$$V_1(Q) = \frac{1}{2}\omega^2 Q^2 \tag{28}$$

$$V_2(Q) = \frac{1}{2}\omega^2 (Q - Q_0)^2 + \Delta G \tag{29}$$

with

$$Q_0 = \frac{1}{\omega}\sqrt{2\lambda} \tag{30}$$

The numerical results in comparison with the full dimensional calculations are shown in Figure 13. The effective one-dimensional model based on the present formulation (dash line)

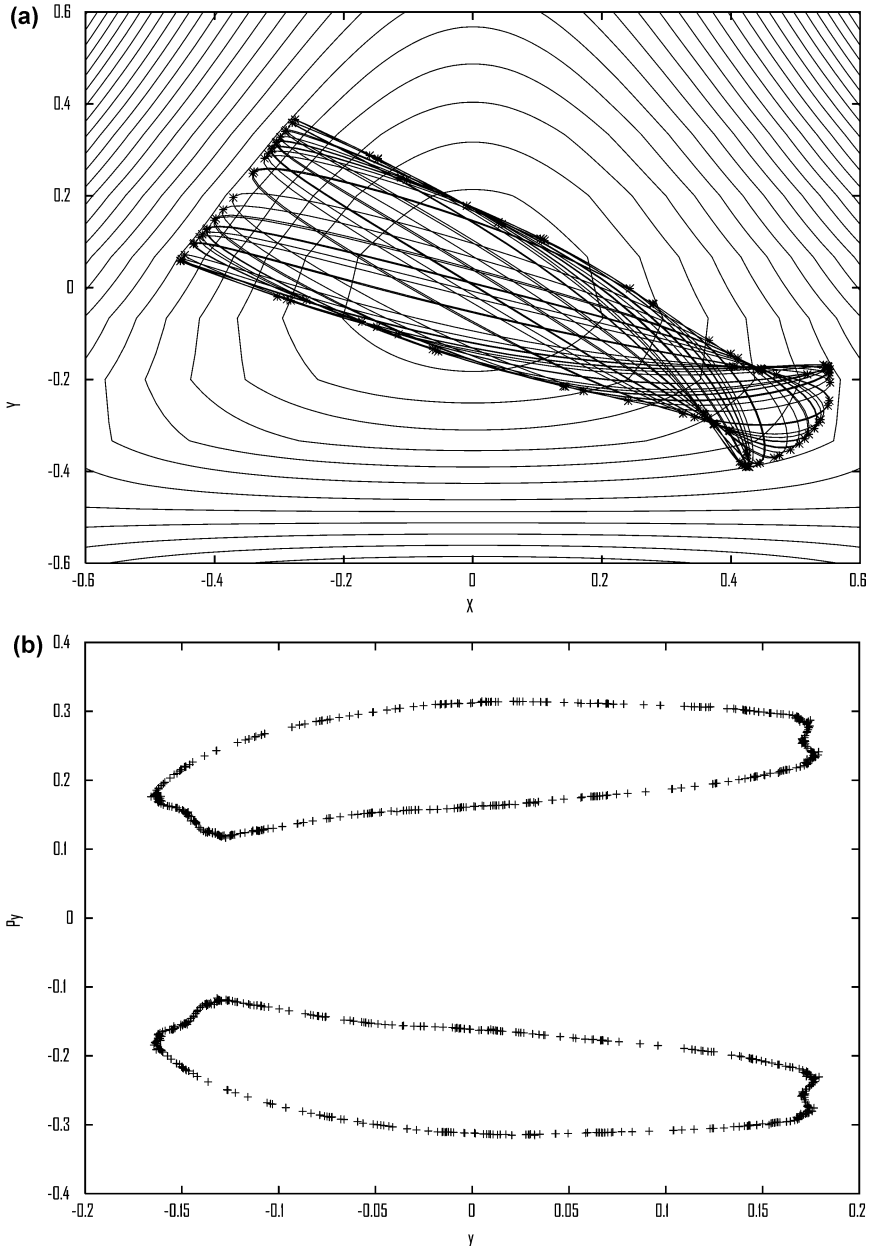

Figure 14. (a) Trajectories and caustics (*) on the Henon−Heiles potential for the initial condition $x_0 = -0.43$ and $y_0 = -0.39$. Partial destruction of regular caustics is seen. (b) Poincare surface corresponding to (a). (a) and (b) reprinted from ref 37. Copyright 2004 World Scientific Publishing Co.

agrees well with the present full dimensional calculations (solid line), indicating the acceptability of the effective one-dimensional model, at least in the case of symmetric potentials. The present results are also compared with the exact quantum mechanical calculations in the one-dimensional flux−flux correlation function approach[47] and are found to be in good agreement with the latter (not shown here).

As demonstrated here, the incorporation of the ZN formulas can very much improve the applicability of the theories of electron transfer. A similar improvement should be carried out in the so-called inverted regime. It should also be noted that the present adiabatic limit is different from the solvent controlled adiabatic limit where the rate saturates in the strong coupling limit and the saturation value is determined by the dielectric relaxation time.[50] The present treatment should thus be extended so as to take into account the effects of solvent dynamics. These studies are now in progress.

V. Inclusion of Tunneling Effect

Needless to say, tunneling is the most well-known quantum mechanical effect, and it is naturally desirable to take the effect into account by using classical trajectories. Generally speaking, there are three kinds of problems: (i) energy splitting in a symmetric double well potential, (ii) decay of metastable state through tunneling, and (iii) tunneling in reaction. For the first two problems we have recently been successful in formulating a practically useful method applicable to realistic polyatomic molecules.[53] This includes an efficient method to carry out the time-consuming accurate ab initio quantum chemical computations of potential energy surfaces. The basic idea is the same as the instanton theory;[54,55] but a very efficient method to find the instanton trajectory has been devised. The method has been applied to real polyatomic molecules and very good agreements are obtained with the experiments.[53] The detailed discussions

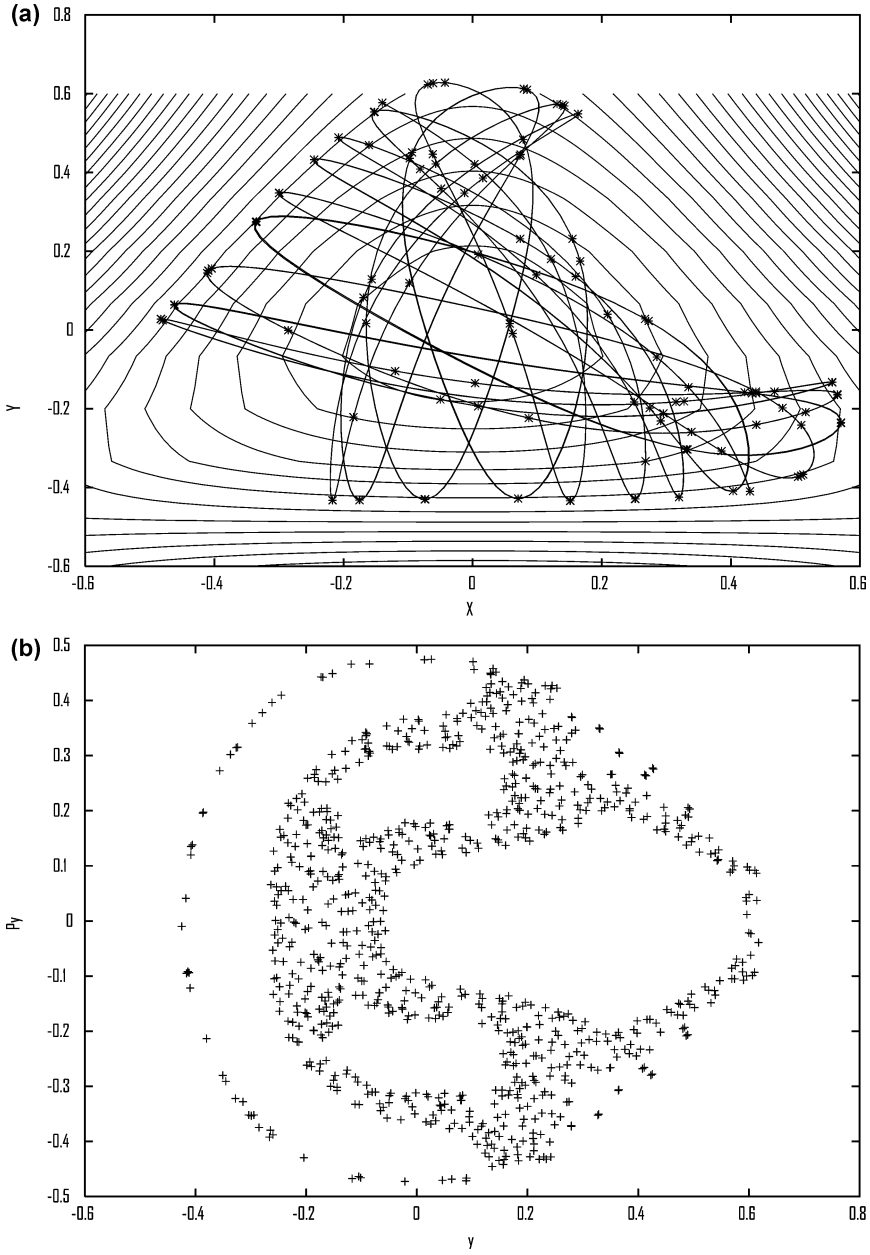

Figure 15. (a) Trajectories and caustics (*) on the Henon−Heiles potential for the initial condition $x_0 = -0.43$ and $y_0 = -0.41$. The classical dynamics is chaotic. (b) Poincare surface corresponding to (a). Torus is totally destroyed. (a) and (b) reprinted with permission from ref 37. Copyright 2004 World Scientific Publishing Co.

are not given here, however, and the reader should refer to ref 53. Instead, the third problem mentioned above is discussed here.

Naturally, numerous works have been done by many authors to deal with tunneling in chemical reactions such as the classical **S** matrix theory,[56] various versions of transition state theory,[57] and the anti-Newtonian mechanics.[58] Here we consider a possible extension of the ZN-TSH method mentioned in section III or the semiclassical method in section II. This means that it is desirable, first of all, to devise a method to efficiently detect caustics along classical trajectories in real coordinate space, because the caustics provide the position for a tunneling trajectory to emanate into a classically forbidden space. Recently, an efficient method has been proposed to locate caustics of classical trajectories on-the-fly.[37] One such approach has been proposed before to propagate $\partial q(t)/\partial q(0)$, which is a minor of the monodromy matrix,[59,60] where $q(t)$ is a time-dependent generalized coordinate. We believe, however, that the present method is much more stable than theirs, because their final differential equation to be solved is second-order and the solutions may become unstable due to exponentially growing and decaying terms.

Our approach is to propagate $\partial p(t)/\partial q(t)$, which is a solution of the Riccati-type nonlinear differential equation as described below. At caustics this quantity diverges so that an appropriate transformation is required to detect caustics. In a $2N$-dimensional phase space, the N-dimensional Lagrange manifold is formed by a continuous set of the trajectories $\{q(t), p(t)\}$. In this manifold the matrix composed of

$$A_{ij} = \frac{\partial p_i}{\partial q_j} \qquad i.j = 1, 2, ..., N \tag{31}$$

satisfies the following Riccati-type differential equation along the classical trajectory:

$$\frac{\partial A}{\partial t} = -H_{qq} - H_{qp}A - AH_{pq} - AH_{pp}A \tag{32}$$

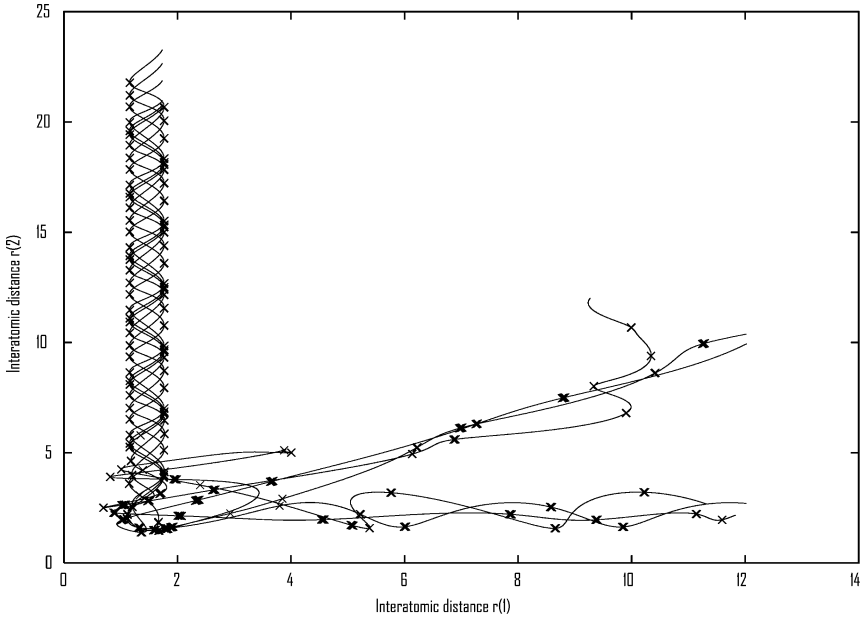

Figure 16. Family of reactive trajectories and caustics (x) on the ground adiabatic potential energy surface of the model CH_2. Reprinted with permission from ref 37. Copyright 2004 World Scientific Publishing Co.

where H_{qq}, H_{qp}, etc. are the matrixes of the second derivative of the classical Hamiltonian taken along the trajectory, i.e., $H_{qq} = \partial^2 H/\partial q \partial q$, etc. At caustics the solution of this differential equation diverges

$$\mathrm{Det}|\mathbf{A}(t_{\mathrm{caustics}})| = \infty \tag{33}$$

Beyond this point further solution of the differential equation is not possible; beisdes, it is not appropriate to detect the caustics accurately from the divergence. So it is necessary to make an appropriate transformation to the matrix **A**. To clarify the basic idea, let us consider the one-dimensional case for the moment. At the turning point $p(q) = 0$ and **A** diverges. By inverting **A** to $\tilde{\mathbf{A}} = \partial q/\partial p$, one eliminates the divergence and the propagation of $\tilde{\mathbf{A}}$ proceeds smoothly through caustics with the zero detected as the caustics. This inversion transformation is equivalent to the canonical transformation: $(p, q) \rightarrow (-\tilde{q}, \tilde{p})$. Equation 32 does not change under this transformation. A useful approach in the *N*-dimensional case is to invert only the diverging element(s) of the matrix. Suppose the diverging element is A_{NN}, the transformation $(p_{\mathrm{N}}, q_{\mathrm{N}}) \rightarrow (-\tilde{q}_{\mathrm{N}}, \tilde{p}_{\mathrm{N}})$ is made. Once the propagation runs through the divergent region and the caustics is detected, the inverse transformation is applied in exactly the reverse order to resume the propagation further. The fourth-order Adams−Bashforth−Moulton predictor−corrector scheme is used to solve the differential equation and the procedure is confirmed to be quite stable, although some care should be taken in choosing the time step not to miss closely occurring caustics.

The above method has been applied to the following two cases: (i) two-dimensional Henon-Heiles potential and (ii) three-dimensional chemical reaction in a model CH_2 system for *J* (total angular momentum) = 0.[37] The Henon−Heiles potential used is as follows (in atomic units):

$$H = \frac{1}{2}(p_x^2 + p_y^2) + \frac{1}{2}(x^2 + y^2) + \left(x^2 y - \frac{1}{3}y^3\right) \tag{34}$$

The classical trajectory is generated from the turning point $\mathbf{p}(0) = 0$, which corresponds to the initial condition $A^{-1} = 0$. After a short time propagation of A^{-1} the propagation is continued with the matrix **A**. Figures 14 and 15 show the results. The initial conditions are $(x_0, y_0) = (-0.43, -0.39)$ for Figure 14 and $(-0.43, -0.41)$ for Figure 15. Figure 14 (15) corresponds to a somewhat irregular (chaotic) case. In the regular case the caustics appear along the envelope of the family of trajectories (see Figure 14a), whereas the caustics are distributed rather randomly with the tori totally destroyed as the system becomes chaotic, as seen in Figure 15a. The Poincare surface section shows discontinuities and separatrices (Figure 15b). The present method works well even in such chaotic cases. Figure 16 shows some reactive trajectories together with the caustics along them. The potential energy surface used is the ground adiabatic state obtained from the DIM model of CH_2. The collision energy and the initial rovibrational states are 1.2 eV and $(v = 0, j = 0)$, respectively. The initial condition for the matrix **A** is obtained by using the energy and momentum conservation in the asymptotic region.

Unfortunately, there is no convincingly good theory yet how to run a tunneling trajectory from the caustics. An extension of the ordinary WKB type solution into the classically forbidden region was discussed by Takada and Nakamura[61] with use of the one-dimensional connection formulas in the vicinity of caustics to connect the wave functions between classically allowed and forbidden regions. However, this cannot be practical for multidimensional systems higher than two dimensions, unfortunately. The anti-Newtonian mechanics, on the other hand, has been considered by Takatsuka and co-workers;[58] but the formulation is not symmmetric with respect to the generalized corrdinates and momenta, as it should be, unfortunately, and formally cannot be correct. Some simple trajectories such as straight lines, however, have been used quite often in practical computations, and they are actually found to work relatively well.[62] This simple idea of straight line trajectories starting from the caustics normal to the classical trajectory has been applied to calculate the thermal rate constant in the H_3 system.[63] The results are shown in Figure 17. The results with tunneling included agree well with the quantum mechanical transition state theory calculations, although it is not shown here.

As this example demonstrates, the important quantum mechanical tunneling effect can also be simply incorporated into the methods explained in sections II and III. Especially, the ZN-

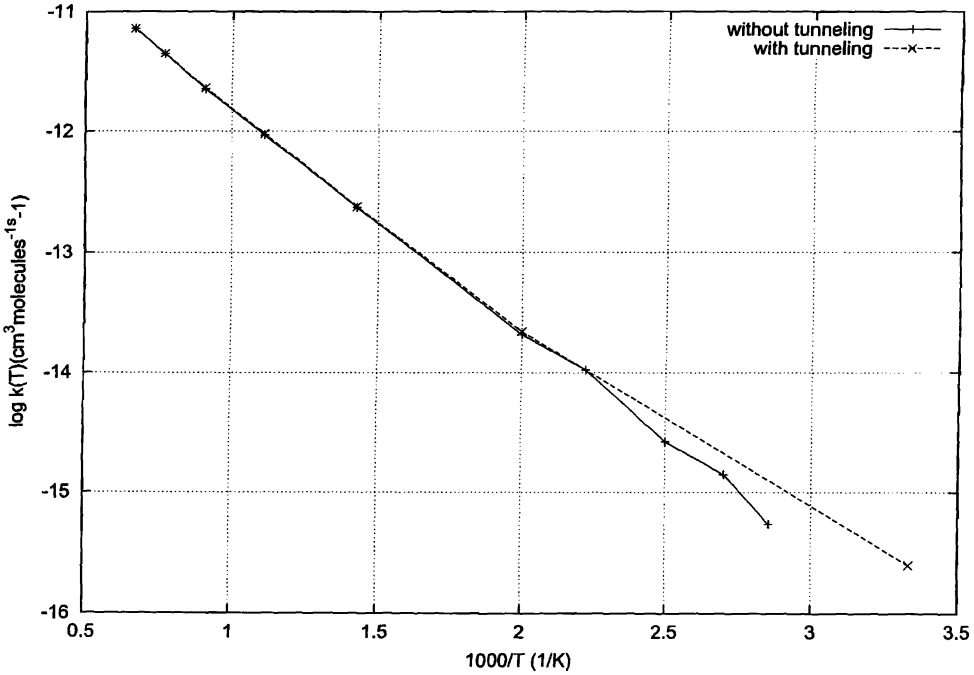

Figure 17. Thermal reaction rate constant of H_3. Solid line: without tunneling Dotted line: with tunneling.

TSH method can incorporate the nonadiabatic transition and the tunneling simply by running trajectories.

VI. Concluding Remarks

Nonadiabatic transitions due to potential energy surface crossings are definitely playing crucial roles in various kinds of chemical processes. They (i) are important to comprehend the mechanisms of chemical dynamics occurring in nature, (ii) provide us guiding principles how to improve the efficiencies of the dynamics, (iii) present useful tools to control the reactions by using external fields such as lasers, and (iv) play key roles to manifest and create new functions of molecules. The Zhu−Nakamura (ZN) theory presents a set of analytical formulas to describe the dynamics in the potential curve-crossing problems and can play basic roles in the studies mentioned above. Although the theory is a one-dimensional one, it works well mainly because the nonadiabatic coupling is a vector defined in multidimensional space.

In this Feature Article, the above subject (i) has been picked up and the developments of new semiclassical methods with the ZN formulas incorporated and their applications to various dynamic processes have been explained and discussed on the basis of the recent activities done in the author's research group. The semiclassical frozen Gaussian wave packet propagation method based on the Herman−Kluk type of formulation and the generalized TSH (trajectory surface hopping) method can now be applied to realistic large systems. The classically forbidden nonadiabatic transitions, which play significant roles in many cases can be treated properly. Quantum mechanical tunneling effects can also be taken into account in these treatments by detecting the caustics along the classical trajectories. Obviously, the frozen Gaussian wave packet propagation method is more accurate than the TSH method. The generalized TSH method would be, however, quite useful and convenient to obtain some averaged physical quantities and to qualitatively comprehend the mechanisms of large systems, if the very much detailed information is not required.

The nonadiabatic transition state theory is formulated and the direct evaluation of thermal rate constant of nonadiabatic chemical reactions becomes possible, although a further generalization of the formulation is necessary so that we can treat a general case that the potential surface crossing and the transition state are separated. Electron transfer is another important subject, because it plays crucial roles in various chemical and biological systems. As a sort of first step, the famous Marcus formula has been modified with use of the ZN formulas and the new formula has been found to work well in the whole range of electronic coupling strength. This has been done for the so-called normal case in which the potential surfaces have the nonadiabatic tunneling type crossings. A similar formulation in the inverted case and also the extension of the formulation are necessary so as to include the effects of solvent dynamics.

The other subjects mentioned above such as the manifestation and creation of molecular functions and the laser control of chemical dynamics have not been discussed in this Feature Article. These will be reviewed in near future elsewhere.

VII. Appendix: Zhu−Nakamura Fomluas

Here the final expressions of the Zhu−Nakamura formulas that can be directly applied to practical problems are summarized for the two types of transitions: (1) Landau−Zener type of transition in which the two diabatic potentials have the same sign of slopes and (2) nonadiabatic tunneling type of transition in which the two diabatic potentials have opposite signs of slopes. It should be noted that there are some typographical errors in the expressions given in refs 1 and 11. The necessary corrections are explained in ref 2. The whole set of correct expressions is provided here.

It should be noted that the formulas presented here contain some empirical corrections that have been introduced to cover some small limiting regimes.[1,11,13]

1. Landau−Zener Type of Transition. The two dimensionless basic parameters a^2 and b^2 in terms of the diabatic potentials are defined as

$$a^2 = \frac{\hbar^2}{2m}\frac{F(F_1 - F_2)}{8V_X^3} \quad \text{(A.1)}$$

and

$$b^2 = (E - E_X)\frac{F_1 - F_2}{2FV_X} \quad \text{(A.2)}$$

with $F = \sqrt{|F_1F_2|}$, where F_j (j = 1, 2), V_X, and E_X are the slopes of diabataic potentials, the diabatic coupling, and the energy at the potential crossing, respectively. These parameters can be re-expressed in terms of the adiabatic potentials (E_1 and E_2 with $E_2 > E_1$) as given below. This means that the diabatization of adiabatic potentials are not necessary; besides the transition probabilities can be estimated more accurately with the use of these parameters expressed in terms of adiabatic potentials:

$$a^2 = \sqrt{d^2 - 1}\,\frac{\hbar^2}{m(T_2^0 - T_1^0)^2[E_2(R_0) - E_1(R_0)]} \quad \text{(A.3)}$$

and

$$b^2 = \sqrt{d^2 - 1}\,\frac{2E - [E_2(R_0) + E_1(R_0)]}{[E_2(R_0) - E_1(R_0)]} \quad \text{(A.4)}$$

where

$$d^2 = \frac{[E_2(T_1^0) - E_1(T_1^0)][E_2(T_2^0) - E_1(T_2^0)]}{[E_2(R_0) - E_1(R_0)]^2} \quad \text{(A.5)}$$

The position R_0 corresponds to the minimum separation of the two adiabatic potentials, and T_1^0 and T_2^0 are defined as (see Figure A1)

$$E_X = [E_1(R_0) + E_2(R_0)]/2 = E_1(T_1^0) = E_2(T_2^0) \quad \text{(A.6)}$$

In terms of the Stokes constant U_1 the reduced scattering matrix S^R can be quantum mechanically exactly given by

$$S^R = \begin{pmatrix} (1 + U_1U_2)\exp(-2i\sigma) & -U_2 \\ -U_2 & (1 - U_1^*U_2)\exp(2i\sigma) \end{pmatrix} \quad \text{(A.7)}$$

where

$$U_2 = \frac{U_1 - U_1^*}{1 + |U_1|^2} \quad \text{(A.8)}$$

The overall nonadiabatic transition probability between the two adiabatic states is given by

$$P_{12} = |S_{12}^R|^2 = \frac{4(\mathrm{Im}\ U_1)^2}{(1 + |U_1|^2)^2} = 4p(1 - p)\sin^2\psi \quad \text{(A.9)}$$

with

$$\psi = \arg(U_1) \quad \text{(A.10)}$$

and

$$p = \frac{1}{1 + |U_1|^2} \quad \text{(A.11)}$$

where p represents the nonadiabatic transition probability for one passage of the crossing point. It should be noted that the above expressions are quantum mechanically *exact* as far as the Stokes constant U_1 is exact. Below, the semiclassical expressions in the Zhu−Nakamura theory are given.

1.1. Case A: $E \geq E_X$. The Stokes constant U_1, which is actually a function of the parameters is given as

$$U_1 = \sqrt{\frac{1}{p} - 1}\,\exp(i\psi) \quad \text{(A.12)}$$

where

$$p = \exp\left[-\frac{\pi}{4a}\left(\frac{2}{b^2 + \sqrt{b^4 + 0.4a^2 + 0.7}}\right)^{1/2}\right] \quad \text{(A.13)}$$

and

$$\psi = \sigma + \phi_S = \sigma - \frac{\delta_\psi}{\pi} + \frac{\delta_\psi}{\pi}\ln\left(\frac{\delta_\psi}{\pi}\right) - \arg\Gamma\left(i\frac{\delta_\psi}{\pi}\right) - \frac{\pi}{4} \quad \text{(A.14)}$$

The parameters σ and δ are defined below in section 1.3. The nonadiabatic transition amplitude, which connects the wave function just before and right after the transition at the avoided crossing is given by

$$I_X = \begin{pmatrix} \sqrt{1 - p}\exp(i\phi_S) & -\sqrt{p}\exp(i\sigma_0) \\ \sqrt{p}\exp(-i\sigma_0) & \sqrt{1 - p}\exp(-i\phi_S) \end{pmatrix} \quad \text{(A.15)}$$

1.2. Case B: $E \leq E_X$. The Stokes constant U_1 is given by

$$\mathrm{Re}\ U_1 = \cos(\sigma)\left\{\sqrt{B(\sigma/\pi)}\exp(\delta) - g_1\sin^2(\sigma)\frac{\exp(-\delta)}{\sqrt{B(\sigma/\pi)}}\right\} \quad \text{(A.16)}$$

and

$$\mathrm{Im}\ U_1 = \sin(\sigma)\left\{B(\sigma/\pi)\exp(2\delta) - g_1^2\sin^2(\sigma) \times \cos^2(\sigma)\frac{\exp(-2\delta)}{B(\sigma/\pi)} + 2g_1\cos^2(\sigma) - g_2\right\}^{1/2} \quad \text{(A.17)}$$

The probability p is given by

$$p = [1 + B(\sigma/\pi)\exp(2\delta) - g_2\sin^2(\sigma)]^{-1} \quad \text{(A.18)}$$

where

$$g_1 = 1.8(a^2)^{0.23}\exp(-\delta) \quad \text{(A.19)}$$

$$g_2 = \frac{3\sigma}{\pi\delta}\ln(1.2 + a^2) - \frac{1}{a^2} \quad \text{(A.20)}$$

and

$$B(X) = \frac{2\pi X^{2X}\exp(-2X)}{X\Gamma^2(X)} \quad \text{(A.21)}$$

1.3. Definitions of σ, δ, and δ_ψ. These parameters introduced above are defined here. The expressions of σ and δ are dependent on the energy as described below. Because σ_0 and δ_0, which appear below, and the parameter δ_ψ are common in the all energy regions, these are defined first.

$$\delta_\psi = \delta\left(1 + \frac{5a^{1/2}}{a^{1/2} + 0.8}10^{-\sigma}\right) \quad \text{(A.22)}$$

$$\sigma_0 + \mathrm{i}\delta_0 \equiv \int_{R_0}^{R_*}[K_1(R) - K_2(R)]\,\mathrm{d}R \simeq \frac{\sqrt{2}\pi}{4a}\frac{F_-^{\mathrm{c}} + \mathrm{i}F_+^{\mathrm{c}}}{{F_+}^2 + {F_-}^2} \quad \text{(A.23)}$$

where

$$F_\pm = \sqrt{\sqrt{(b^2+\gamma_1)^2+\gamma_2} \pm (b^2+\gamma_1)} + \sqrt{\sqrt{(b^2-\gamma_1)^2+\gamma_2} \pm (b^2-\gamma_1)} \quad \text{(A.24)}$$

$$F_+^{\mathrm{c}} = F_+[b^2 \rightarrow (b^2 - {b_{\mathrm{c}}}^2)] \quad \text{(A.25)}$$

$$F_-^{\mathrm{c}} = F_-(\gamma_2 \rightarrow \gamma_2') \quad \text{(A.26)}$$

$$\gamma_1 = 0.9\sqrt{d^2 - 1} \quad \text{(A.27)}$$

and

$$\gamma_2 = \frac{7}{16}\sqrt{d^2} \quad \text{(A.28)}$$

with

$${b_{\mathrm{c}}}^2 = \frac{0.16 b_{\mathrm{x}}}{\sqrt{1+b^4}} \quad \text{(A.29)}$$

$$\gamma_2' = \frac{0.45\sqrt{d^2}}{1 + 1.5\exp(2.2 b_x |b_x|^{0.57})} \quad \text{(A.30)}$$

and

$$b_x = b^2 - 0.9553 \quad \text{(A.31)}$$

Now, σ and δ are given:

(a) When $E \geq E_2(R_0)$,

$$\sigma = \int_{T_1}^{R_0} K_1(R)\,\mathrm{d}R - \int_{T_2}^{R_0} K_2(R)\,\mathrm{d}R + \sigma_0 \quad \text{(A.32)}$$

and

$$\delta = \delta_0 \quad \text{(A.33)}$$

(b) When $E \leq E_1(R_0)$,

$$\sigma = \sigma_0 \quad \text{(A.34)}$$

and

$$\delta = -\int_{R_0}^{T_1} |K_1(R)|\,\mathrm{d}R + \int_{R_0}^{T_2} |K_2(R)|\,\mathrm{d}R + \delta_0 \quad \text{(A.35)}$$

(c) When $E_1(R_0) < E < E_2(R_0)$,

$$\sigma = \int_{T_1}^{R_0} K_1(R)\,\mathrm{d}R + \sigma_0 \quad \text{(A.36)}$$

and

$$\delta = \int_{R_0}^{T_2} K_2(R)\,\mathrm{d}R + \delta_0 \quad \text{(A.37)}$$

2. Nonadiabatic Tunneling Type of Transition. The two parameters a^2 and b^2 in terms of diabatic potentials are the same as eqs A.1 and A.2. In terms of adiabatic potentials, however, they are differently defined as

$$a^2 = \frac{(1-\gamma^2)\hbar^2}{m(R_{\mathrm{b}} - R_{\mathrm{t}})^2(E_{\mathrm{b}} - E_{\mathrm{t}})} \quad \text{(A.38)}$$

and

$$b^2 = \frac{2E - (E_{\mathrm{b}} + E_{\mathrm{t}})}{E_{\mathrm{b}} - E_{\mathrm{t}}} \quad \text{(A.39)}$$

where

$$\gamma = \frac{E_{\mathrm{b}} - E_{\mathrm{t}}}{E_2\left(\frac{R_{\mathrm{b}} + R_{\mathrm{t}}}{2}\right) - E_1\left(\frac{R_{\mathrm{b}} + R_{\mathrm{t}}}{2}\right)} \quad \text{(A.40)}$$

The reduced scattering matrix in terms of the Stokes constant U_1 is given quantum mechanically exactly as

$$S^{\mathrm{R}} = \frac{1}{1 + U_1 U_2}\begin{pmatrix} \exp(\mathrm{i}\Delta_{11}) & U_2\exp(\mathrm{i}\Delta_{12}) \\ U_2\exp(\mathrm{i}\Delta_{12}) & \exp(\mathrm{i}\Delta_{22}) \end{pmatrix} \quad \text{(A.41)}$$

where

$$U_2 = \frac{U_1 - U_1^*}{|U_1|^2 - 1} \quad \text{(A.42)}$$

It should be noted that the Stokes constants are naturally different from those in the Landau−Zener type of transition. R_{t} and E_{t} (R_{b} and E_{b}) represent the position and energy of the top (bottom) of the lower (upper) adiabatic potential (see Figure 18). The suffixes 1 and 2 of the **S** matrix designate not the adiabatic potential, but the regions in coordinate space with respect to the potential crossing. Namely, the off-diagonal element S_{12} represents the transmission through the crossing region. When the adiabatic potentials are symmetric around the crossing point and $R_{\mathrm{t}} = R_{\mathrm{b}}$ is satisfied, γ becoms unity and the appropriate limit should be taken to define the parameter a^2, which gives

$$a^2 = \frac{\hbar^2}{4m(E_{\mathrm{b}} - E_{\mathrm{t}})^2}\left[\left.\frac{\partial^2 E_2(R)}{\partial R^2}\right|_{R=R_{\mathrm{b}}} - \left.\frac{\partial^2 E_1(R)}{\partial R^2}\right|_{R=R_{\mathrm{t}}}\right] \quad \text{(A.43)}$$

The semiclassical expressions in the Zhu−Nakamura theory are given below for the Stokes constant and other important physical quantities.

2.1. Case A: $E \geq E_{\mathrm{b}}$. The Stokes cosntant U_1 is given by

$$U_1 = \mathrm{i}\sqrt{1-p}\,\exp(\mathrm{i}\psi) \quad \text{(A.44)}$$

where the nonadiabatic transition probability p for one-passage of the crossing point and the phase ψ are defined as

$$p = \exp\left[-\frac{\pi}{4a}\left(\frac{2}{b^2 + \sqrt{b^4 - 0.72 + 0.62a^{1.43}}}\right)\right] \quad \text{(A.45)}$$

and

$$\psi = \sigma - \phi_{\mathrm{S}} = \sigma + \frac{\delta}{\pi} - \frac{\delta}{\pi}\ln\left(\frac{\delta}{\pi}\right) + \arg\Gamma\left(\mathrm{i}\frac{\delta}{\pi}\right) + \frac{\pi}{4} - g_7 \quad \text{(A.46)}$$

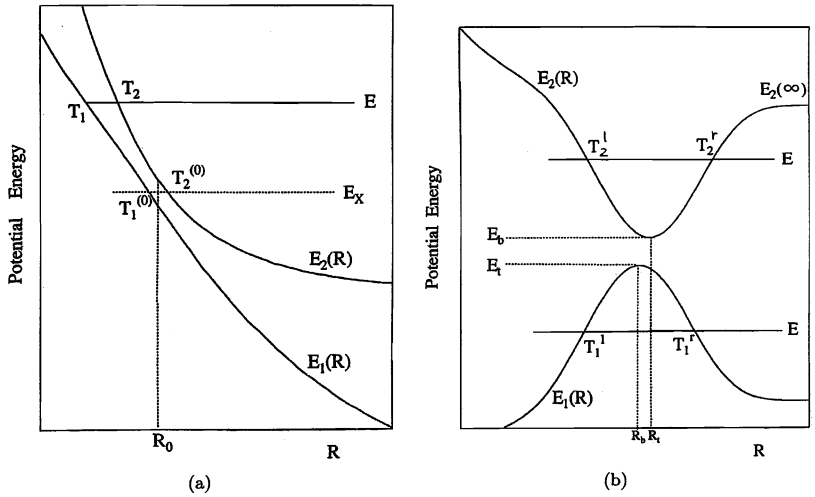

Figure 18. Schematic adiabatic potentials and various parameters used in the ZN formulas for (a) Landau−Zener case and (b) nonadiabatic tunneling case.

with

$$\sigma = \int_{T_2^l}^{T_2^r} K_2(R)\,\mathrm{d}R \tag{A.47}$$

$$\delta = \frac{\pi}{16ab}\frac{\sqrt{6+10\sqrt{1-b^{-4}}}}{1+\sqrt{1-b^{-4}}} \tag{A.48}$$

and

$$g_7 = \frac{0.23a^{1/2}}{a^{1/2}+0.75}40^{-\sigma} \tag{A.49}$$

The phases appearing in the definition of **S** matrix are given as

$$\Delta_{11} = 2\int_{T_2^l}^{R_b} K_2(R)\,\mathrm{d}R - 2\sigma_0 \tag{A.50}$$

$$\Delta_{22} = 2\int_{R_b}^{T_2^r} K_2(R)\,\mathrm{d}R + 2\sigma_0 \tag{A.51}$$

$$\Delta_{12} = \sigma \tag{A.52}$$

with

$$\sigma_0 = \frac{R_b - R_t}{2}\left[K_1(R_t) + K_2(R_b) + \frac{[K_1(R_t) - K_2(R_b)]^2}{3[K_1(R_t) + K_2(R_b)]}\right] \tag{A.53}$$

T_2^r and T_2^l are the turning points on $E_2(R)$ (see Figure 18). The nonadiabatic transition amplitude to connect the wave functions between the right and the left sides of the crossing point is given by

$$I_X = \begin{pmatrix} \sqrt{1-p}\exp(i\phi_S) & \sqrt{p}\exp(i\sigma_0) \\ -\sqrt{p}\exp(-i\sigma_0) & \sqrt{1-p}\exp(-i\phi_S) \end{pmatrix} \tag{A.54}$$

The overall transmission probability from the left to the right or vice versa is given by

$$P_{12} = \frac{4\cos^2(\psi)}{4\cos^2(\psi) + p^2/(1-p)} \tag{A.55}$$

2.2. Case B: $E_b \geq E \geq E_t$. The Stokes constant U_1 is given by

$$U_1 = i[\sqrt{1+W^2}\exp(i\phi) - 1]/W \tag{A.56}$$

with

$$W = \frac{1+g_5}{a^{2/3}}\int_0^\infty \cos\left[\frac{t^3}{3} - \frac{b^2}{a^{2/3}}t - \frac{g_4}{a^{2/3}}\frac{t}{0.61\sqrt{2+b^2}+a^{1/3}t}\right]\mathrm{d}t \tag{A.57}$$

and

$$\phi = \sigma + \arg\Gamma(1/2 + i\delta/\pi) - \frac{\delta}{\pi}\ln\left(\frac{\delta}{\pi}\right) + \frac{\delta}{\pi} - g_3 \tag{A.58}$$

where

$$\sigma = -\frac{(1-b^2)\sqrt{5+3b^2}}{\sqrt{a^2}}\left[0.057(1+b^2)^{0.25} + \frac{1}{3}\right] \tag{A.59}$$

$$\delta = \frac{(1+b^2)\sqrt{5-3b^2}}{\sqrt{a^2}}\left[0.057(1-b^2)^{0.25} + \frac{1}{3}\right] \tag{A.60}$$

$$g_3 = \frac{0.34a^{0.7}(a^{0.7}+0.35)(0.42+b^2)}{a^{2.1}+0.73}\left(2 + \frac{100b^2}{100+a^2}\right)^{0.25} \tag{A.61}$$

$$g_4 = \frac{\sqrt{a^2-3b^2}}{\sqrt{a^2}+3}\sqrt{1.23+b^2} \tag{A.62}$$

and

$$g_5 = 0.38(1+b^2)^{1.2-0.4b^2}/a^2 \tag{A.63}$$

The phases appearing in the definition of **S** matrix are defined as

$$\Delta_{11} = \sigma - 2\sigma_0 \tag{A.64}$$

$$\Delta_{22} = \sigma + 2\sigma_0 \tag{A.65}$$

$$\Delta_{12} = \sigma \tag{A.66}$$

and

$$\sigma_0 = -\frac{1}{3}(R_t - R_b)K_1(R_t)(1 + b^2) \quad \text{(A.67)}$$

The overall transmission probability takes the form

$$P_{12} = \frac{W^2}{1 + W^2} \quad \text{(A.68)}$$

2.3. Case C: $E \leq E_t$. The Stokes constant U_1 is given by

$$\text{Re } U_1 = \sin(2\sigma)\left[\frac{0.5\sqrt{a^2}}{1 + \sqrt{a^2}}\sqrt{B(\sigma_c/\pi)}\exp(-\delta) + \frac{\exp(\delta)}{\sqrt{B(\sigma_c/\pi)}}\right] \quad \text{(A.69)}$$

and

$$\text{Im } U_1 = \cos(2\sigma_c)\sqrt{\frac{(\text{Re } U_1)^2}{\sin^2(2\sigma_c)} + \frac{1}{\cos^2(2\sigma_c)}} - \frac{1}{2\sin(\sigma_c)}\left|\frac{\text{Re } U_1}{\cos(\sigma_c)}\right| \quad \text{(A.70)}$$

where

$$\sigma_c = \sigma(1 - g_6) \quad \text{(A.71)}$$

$$\sigma = \frac{\pi}{16a|b|}\frac{\sqrt{6 + 10\sqrt{1 - b^{-4}}}}{1 + \sqrt{1 - b^{-4}}} \quad \text{(A.72)}$$

$$\delta = \int_{T_1^l}^{T_1^r}|K_1(R)|\,dR \quad \text{(A.73)}$$

and

$$g_6 = 0.32 \times 10^{-2/a^2}\exp(-\delta) \quad \text{(A.74)}$$

T_1^r and T_1^l are the turning points on $E_1(R)$ (see Figure 18). The phase appearing in the definition of **S** matrix are

$$\Delta_{11} = \Delta_{22} = \Delta_{12} = -2\sigma \quad \text{(A.75)}$$

In this energy region physically meaningful quantities are the overall transmission and reflection probabilities. The transmission probability is given by

$$P_{12} = \frac{B(\sigma_c/\pi)\exp(-2\delta)}{\left[1 + \frac{0.5\sqrt{a^2}}{1 + \sqrt{a^2}}B(\sigma_c/\pi)\exp(-2\delta)\right]^2 + B(\sigma_c/\pi)\exp(-2\delta)} \quad \text{(A.76)}$$

This expression contains both effects of quantum mechanical tunneling ($\exp[-2\delta]$ is the Gamov factor) and nonadiabatic transition, which is represented by the factor σ_c. This transmission probability is always smaller than the ordinary tunneling probability through the lower adiabatic potential with the nonadiabatic coupling effect neglected. When the diabatic coupling is infinitely strong, namely, $a^2 \rightarrow 0$, the above transmission probability goes to the ordinary potential penetration probability $= \exp(-2\delta)/[1 + \exp(-2\delta)]$.

Acknowledgment. I thank all the group members in the past and present who carried out all the researches mentioned here: Drs. C. Zhu, G. V. Mil'nikov, Y. Teranishi, K. Nagaya, A. Kondorskiy, H. Fujisaki, S. Chikazumi, S. Zou, H. Tamura, and P. Oloyede. I am indebted to Professors S. Nanbu and T. Ishida for the collaboration on molecular functions and electronic structure calculations. I also thank Professor Y. Zhao for his work on the nonadiabatic transition state theory and electron transfer. The work was supported by a Grant-in-Aid for Specially Promoted Research on "Studies of Nonadiabatic Chemical Dynamics based on the Zhu−Nakamura Theory" from MEXT of Japan.

References and Notes

(1) Nakamura, H. *Nonadiabatic Transition: Concepts, Basic Theories and Applications*; World Scientific: Singapore, 2002.
(2) Nakamura, H. *J. Theo. Comput. Chem.* **2005**, *4*, 127.
(3) Nikitin, E. E.; Umanskii, S. Ya. *Theory of Slow Atomic Collisions*; Springer: Berlin, 1984.
(4) Child, M. S. *Molecular Collision Theory*; Academic Press: London, 1974.
(5) Medevedev, E. S.; Osherov, V. I. *Radiationless Transitions in Polyatomic Molecules*; Springrer Series in Chemical Physics, Vol. 57; Springer: Berlin, 1994.
(6) Tully, J. C. In *Dynamics of Moleculear Collisions, Part B*; Miller, W. H., Ed.; Plenum: New York, 1976.
(7) Michl, J.; Bonacic-Koutecky, V. *Electronic Aspects of Organic Photochemistry*; John Wiley and Sons: New York, 1990.
(8) Bolton, J. R.; Mataga, N.; McLendon, G. *Electron Transfer in Inorganic, Organic, and Biological Systmes, Advances in Chemistry Series 228*; American Chemical Society: Washington, DC, 1991.
(9) Nakamura, H. In *Dynamics of Molecules and Chemical Reactions*; Wyatt, R. E., Zhang, J. Z. H.; Marcel Dekker: New York, 1996.
(10) Nakamura, H.; Zhu, C. *Comments At. Mol. Phys.* **1996**, *32*, 249.
(11) Zhu, C.; Teranishi, Y.; Nakamura, H. *Adv. Chem. Phys.* **2001**, *117*, 127.
(12) Zhu, C.; Mil'nikov, G.; Nakamura, H. *Modern Trends in Chemical Reaction Dynamics*, Liu, K., Yang, X., Eds.; World Scientific: Singapore, 2004.
(13) Zhu, C.; Nakamura, H. *J. Math. Phys.* **1992**, *33*, 2697. Zhu, C.; Nakamura, H.; Re, N.; Aquilanti, V. *J. Chem. Phys.* **1992**, *97*, 1892. Zhu, C.; Nakamura, H. *J. Chem. Phys.* **1992**, *97*, 8497; **1993**, *98*, 6208; **1994**, *101*, 4855; **1998**, *108*, 7501; **1994**, *101*, 10630; **1995**, *102*, 7448; **1998**, *109*, 4689; **1997**, *106*, 2599; **1997**, *107*, 7839; *Chem. Phys. Lett.* **1996**, *258*, 342; **1997**, *274*, 205; *Comput. Phys. Commun.* **1993**, *74*, 9.
(14) Nanbu, S.; Nakamura, H.; Goodman, F. O. *J. Chem. Phys.* **1997**, *107*, 5445.
(15) Nanbu, S.; Ishida, T.; Nakamura, H. *Chem. Phys.*, in press.
(16) Rice, S. A.; Zhao, M. *Optical Control of Molecular Dynamics*; John Wiley and Sons: New York, 2002.
(17) Bandrauk, A. D. *Molecules in Laser Field*; Marcel Dekker Inc.: New York, 1994.
(18) Brumer, P.; Shapiro, M. *Annu. Rev. Phys. Chem.* **1997**, *48*, 601.
(19) Teranishi, Y.; Nakamura, H. *Phys. Rev. Lett.* **1998**, *81*, 2032.
(20) Zou, S.; Kondorskiy, A.; Mil'nikov, G.; Nakamura, H. *J. Chem. Phys.* **2005**, *122*, 084112.
(21) Kondorskiy, A.; Nakamura, H. *J. Theo. Comput. Chem.* **2005**, *4*, 75; **2005**, *4*, 89.
(22) Zou, S.; Kondorskiy, A.; Mil'nikov, G.; Nakamura, H. In *Progress in Ultrafast Intense Laser Science*; Springer: New York, 2006; Vol. II, Section 5. Kondorskiy, A.; Mil'nikov, G.; Nakmaura, H. In *Progress in Ultrafast Intense Laser Science*; Springer: New York, 2006; Vol. II, Section 6.
(23) Makri, N.; Miller, W. H. *J. Chem. Phys.* **1988**, *89*, 2170. Miller, W. H. *J. Chem. Phys.* **1970**, *53*, 3578, **1991**, *95*, 9428. Sun, X.; Miller, W. H. *J. Chem. Phys.* **1997**, *106*, 6346. Miller, W. H. *J. Phys. Chem.* **2001**, *105*, 2942.
(24) Voorhis, T. V.; Heller, E. J. *Phys. Rev.* **2002**, *A66*, 050501. Heller, E. J. *J. Chem. Phys.* **1981**, *75*, 2923.
(25) Herman, M. F.; Kluk, E. *Chem. Phys.* **1984**, *91*, 27. Kluk, E.; Herman, M. F.; Davis, H. D. *J. Chem. Phys.* **1986**, *84*, 326. Herman, M. F. *Annu. Rev. Phys. Chem.* **1994**, *45*, 83.
(26) Walton, A. R.; Manolopoulos, D. E. *Mol. Phys.* **1996**, *87*, 961. Brewer, M. L.; Hulme, J. S.; Manolopoulos, D. E. *J. Chem. Phys.* **1997**, *106*, 4832.
(27) Kondorskiy, A.; Nakamura, H. *J. Chem. Phys.* **2004**, *120*, 8937.
(28) Bjerre, A.; Nikitin, E. E. *Chem. Phys. Lett.* **1967**, *1*, 179.
(29) Tully, J. C.; Preston, R. *J. Chem. Phys.* **1970**, *54*, 4297.
(30) Tully, J. C. *J. Chem. Phys.* **1990**, *93*, 1061.
(31) Toplar, M. S.; Allison, T. C.; Schenke, D. W.; Truhlar, D. G. *J. Phys. Chem. A* **1998**, *102*, 1666. Volobuev, Y.L.; Hack, M.D.; Truhlar,

D.G. *J. Phys. Chem. A* **1999**, *103*, 6309. Hack, M. D.; Jasper, A.; Volobuev, Y. L.; Schwenke, D.; Truhlar, D. G. *J. Phys. Chem. A* **2000**, *104*, 217. Volobuev, Y. L.; Hack, M. D.; Toplar, M.; Truhlar, D. G. *J. Chem. Phys.* **2000**, *112*, 9716. Jasper, A.; Hack, M. D.; Truhlar, D. G. *J. Chem. Phys.* **2001**, *115*, 1804. Hack, M. D.; Truhlar, D. G. *J. Chem. Phys.* **2001**, *114*, 2894.

(32) Tully, J. C. In *Modern Methods for MultidimensionalDynamics Computations in Chemsitry*; Thompson, D. L., Ed.; World Scientific: Singapore, 1998.

(33) Domcke, W.; Yarkony, D.; Koppel, H. *Conical Intersections, Electronic Structures, Dynamics and Spectroscopy*; World Scientific: Singapore, 2004.

(34) Jasper, A.; Kendrick, B. K.; Mead, C. A.; Truhlar, D. G. In *Modern Trends in Chemical Reaction Dynamics: Experiment and Theory*; Yang, X., Liu, K. Eds.; World Scientific: Singapore, 2004.

(35) Zhao, Y.; Mil'nikov, G.; Nakamura, H. *J. Chem. Phys.* **2004**, *121*, 8854.

(36) Zhao, Y.; Lia, W.; Nakamura, H. *J. Phys. Chem. A* **2006**, *110*, 8204.

(37) Oloyede, P.; Mil'nikov, G.; Nakamura, H. *J. Theo. Comput. Chem.* **2004**, *3*, 91.

(38) Kondorskiy, A.; Nakamura, H. *J. Theo. Comput. Chem.* **2005**, *4*, 89.

(39) Oloyede, P.; Mil'nikov, G.; Nakamura, H. *J. Chem. Phys.* **2006**, *124*, 144110.

(40) Nagaya, K.; Teranishi, Y.; Nakamura, H. *ACS Symp. Ser.* **2002**, *821*, 98; *J. Chem. Phys.* **2000**, *113*, 6197; **2002**, *117*, 9588.

(41) Kosloff, R.; Rice, S. A.; Gaspard, P.; Tersigni, S.; Tannor, D. J. *Chem. Phys.* **1989**, *139*, 201.

(42) Kondorskiy, A.; Mil'nikov, G.; Nakamura, H. *Phys. Rev.* **2005**, *A72*, 041401.

(43) Zhu, C.; Nobusada, K.; Nakamura, H. *J. Chem. Phys.* **2001**, *115*, 3031. Zhu, C.; Kamisaka, H.; Nakamura, H. *J. Chem. Phys.* **2001**, *115*, 11036; **2002**, *116*, 3234.

(44) Miller, W. H. In *Dynamics of Molecules and Chemical Reactions*; Wyatt, R. E., Zhang, J. Z. H., Eds.; Marcel Dekker: New York, 1996; Chapter 10.

(45) Miller, W. H.; Zhao, Y.; Ceotto, M.; Yang, S. *J. Chem. Phys.* **2003**, *119*, 1329.

(46) Chikazumi, S.; Mil'nikov, G.; Nakamura, H. *1st APACTC (Asian Pacific Conference on Theoretical and Computational Chemistry)* **2004**, Poster 07.

(47) Miller, W. H.; Schwartz, S. D.; Tromp, J. W. *J. Chem. Phys.* **1983**, *79*, 4889.

(48) Shin, C.; Shin, S. *J. Chem. Phys.* **2000**, *113*, 6528.

(49) Marcus, R. A.; Sutin, N. *Biochim. Biophys. Acta* **1985**, *811*, 265.

(50) Barzykin, A. V. G.; Frantsuzov, P. A.; Seki, K.; Tachiya, M. *Adv. Chem. Phys.* **2002**, *123*, 511.

(51) Bixon, M.; Jortner, J. *Adv. Chem. Phys.* **1999**, *106*, 35.

(52) Dogonadze, R. R.; Urushadze, Z. D. *J. Electranal. Chem.* **1971**, *32*, 235.

(53) Mil'nikov, G.; Nakamura, H. *J. Chem. Phys.* **2001**, *115*, 6881; **2002**, *117*, 10081. Mil'nikov, G.; Yagi, K.; Taketsugu, T.; Nakamura, H.; Hirao, K. *J. Chem. Phys.* **2003**, *119*, 10; **2003**, *120*, 5036. Yagi, K.; Mil'nikov, G.; Taketsugu, T.; Hirao, K.; Nakamura, H. *Chem. Phys. Lett.* **2004**, *397*, 435. Mil'nikov, G.; Nakamura, H. *J. Chem. Phys.* **2005**, *122*, 124311. Mil'nikov, G.; Ishida, T.; Nakamura, H. *J. Phys. Chem.*, in press.

(54) Benderskii, V. A.; Makarov, D. E.; Wight, C. A. *Chemical Dynamics at Low Temperatures*; Wiley and Sons: New York, 1994.

(55) Miller, W. H. *J. Chem. Phys.* **1974**, *62*, 1899.

(56) Miller, W. H. *Adv. Chem. Phys.* **1974**, *25*, 69; **1975**, *30*, 77.

(57) Tucker, S. C.; Truhlar, D. G. In *New Theoretical Concepts for Understanding Organic Reactions*; Bertran, J., Csizmadia, I. G., Eds.; Kluwer: Dordrecht, The Netherlands, 1967.

(58) Takatsuka, K.; Ushiyama, H.; Inoue-Ushiyama, A. *Phys. Rep.* **1995**, *322*, 5.

(59) Stuchi, T. J.; Vieira-Martins, R. *Phys. Lett.* **1995**, *A201*, 179.

(60) Ushiyama, H.; Arasaki, Y.; Takatsuka, K. *Chem. Phys. Lett.* **2001**, *346*, 169.

(61) Takada, S.; Nakamura, H. *J. Chem. Phys.* **1994**, *100*, 98.

(62) Makri, N.; Miller, W. H. *J. Chem. Phys.* **1989**, *91*, 4026.

(63) Oloyede, P. Ph.D. Thesis, Graduate University for Advanced Studies, 2006.